Lanthanide Sensitization with Ruthenium Carbon-Rich Complexes and Redox Commutation of Near-IR Luminescence

ARTICLE *in* ORGANOMETALLICS · APRIL 2014

Impact Factor: 4.13 · DOI: 10.1021/om500059d

8 AUTHORS, INCLUDING:

Lucie Norel
Université de Rennes 1
29 PUBLICATIONS **602** CITATIONS
SEE PROFILE

Min Feng
Université de Rennes 1
6 PUBLICATIONS **48** CITATIONS
SEE PROFILE

Olivier Maury
Ecole normale supérieure de Lyon
169 PUBLICATIONS **3,422** CITATIONS
SEE PROFILE

ORGANOMETALLICS

Article

pubs.acs.org/Organometallics

Lanthanide Sensitization with Ruthenium Carbon-Rich Complexes and Redox Commutation of Near-IR Luminescence

Lucie Norel,*[,†] Emmanuel Di Piazza,[†] Min Feng,[†] Antoine Vacher,[†] Xiaoyan He,[†] Thierry Roisnel,[†] Olivier Maury,[‡] and Stéphane Rigaut*[,†]

[†]Institut des Sciences Chimiques de Rennes, UMR 6226 CNRS-Université de Rennes 1, 263 Av. du Général Leclerc, F-35042 Rennes Cedex, France

[‡]Laboratoire de Chimie, UMR 5182, CNRS-Ecole Normale Supérieure de Lyon, 46 allée d'Italie, 69007 Lyon, France

Supporting Information

ABSTRACT: With the help of associations between Eu^{3+}, Yb^{3+}, and Nd^{3+} ions and low-potential redox-active ruthenium carbon-rich complexes bearing bipyridine chelating unit(s) of the type *trans*-[Ph−C≡C−$(dppe)_2$Ru−C≡C−bipy-κ^2N,N'−Ln$(TTA)_3$], *trans*-[$(dppe)_2$Ru(−C≡C−bipy-κ^2N,N'−Ln$(TTA)_3)_2$], and *trans*-[Ph−C≡C−$(dppe)_2$Ru−C≡C−C_6H_4−C≡C−bipy-κ^2N,N'−Yb$(TTA)_3$], we built new original d−f heterometallic complexes. Efficient sensitization in the visible range of the Nd^{3+} and Yb^{3+} near-infrared (NIR) emitters was achieved with the metal−acetylide antenna, while sensitization of the Eu^{3+} ion was not efficient owing to the low energy level of the antenna excited state. The redox properties of these groups also allow for low-potential redox modulation of NIR luminescence of the Yb^{3+} ion and, for the first time, of the Nd^{3+} ion.

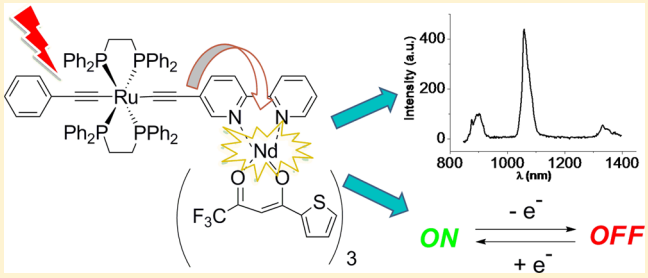

INTRODUCTION

The remote control of a key property with external stimuli in molecular nanosystems is a challenging feature to achieve molecular-based switching devices.[1] It appears that group 8 metal acetylide complexes displaying strong ligand-mediated electronic effects are attractive redox-switchable building blocks for the realization of functional materials.[2−4] Indeed, these transition-metal complexes with direct σ-bond connection of the carbon-rich ligands with the metal atoms show excellent ability to provide a strong electronic interaction between these two components to achieve electrotriggered functional materials, owing to the substantial ligand character of the highest occupied molecular orbital (HOMO) resulting from the overlap of a metal d(π) and of an appropriate π orbital of the carbon-rich ligand.[5] In particular, with ethynyl ruthenium complexes of the type $ClRu(dppe)_2(-C\equiv C-Aryl)$ (dppe = 1,2-bis-(diphenylphosphenyl)ethane), the level of involvement of the carbon-rich ligand in the redox processes is found to be major, with a reduced metal contribution. For instance, such ruthenium acetylides allowed the low-potential redox control of dithienylethene closing to reach unique multifunctional light and electrotriggered molecular junctions.[4] Hence, rational designs with appropriate combinations of such types of organometallics with accurate functional units should lead to the redox perturbations of the targeted molecular properties in a more efficient way than for the ubiquitous ferrocenyl group.[6]

In this context, an interesting target is to use such electroactive units as redox switching antennas for luminescence control of associated emissive units. The remote control of luminescence has attracted considerable interest in investigating new molecular materials and for imaging. This goal can be reached, for example, with the use of photochromic units[7] or with redox-active units.[8,9] In particular, redox modulation of luminescence has been reported for organic compounds[8] or transition-metal complexes[9] through the redox activation/deactivation of the emitter itself or by the creation of a nonradiative pathway via an associated redox center. On the other hand, lanthanide emitters such as Eu, Nd, Yb, and Er with long-lived and narrow bandwidth luminescence,[10] whose lifetimes and quantum yields can be modulated with external perturbations induced by ion or molecules,[11] have been successfully sensitized using d-block metal ions with efficient energy transfer especially through polypyridyl donors, thus lowering the energy needed to the near-UV/vis region by comparison with common organic ligand complexes.[12,13] Some of these works have described the use of redox-active antenna ligands such as ferrocene and tetrathiafulvalene,[14] but surprisingly, until our first preliminary report,[15] redox modulation of luminescence was not achieved with lanthanide ions. In that communication, with the association between an ytterbium ion and a ruthenium acetylide, we obtained the *trans*-[Ph−C≡C−$(dppe)_2$Ru−C≡C−bipy-κ^2N,N'−Yb$(TTA)_3$] (TTA = 2-thenoyltrifluoroacetonate) complex, which enabled the first switching of the near-IR Yb(III) luminescence by taking advantage of

Special Issue: Organometallic Electrochemistry

Received: January 21, 2014
Published: April 24, 2014

   dx.doi.org/10.1021/om500059d | *Organometallics* 2014, 33, 4824−4835

Scheme 1. Synthetic Pathways Yielding the Acetylide Heterometallic Complexes

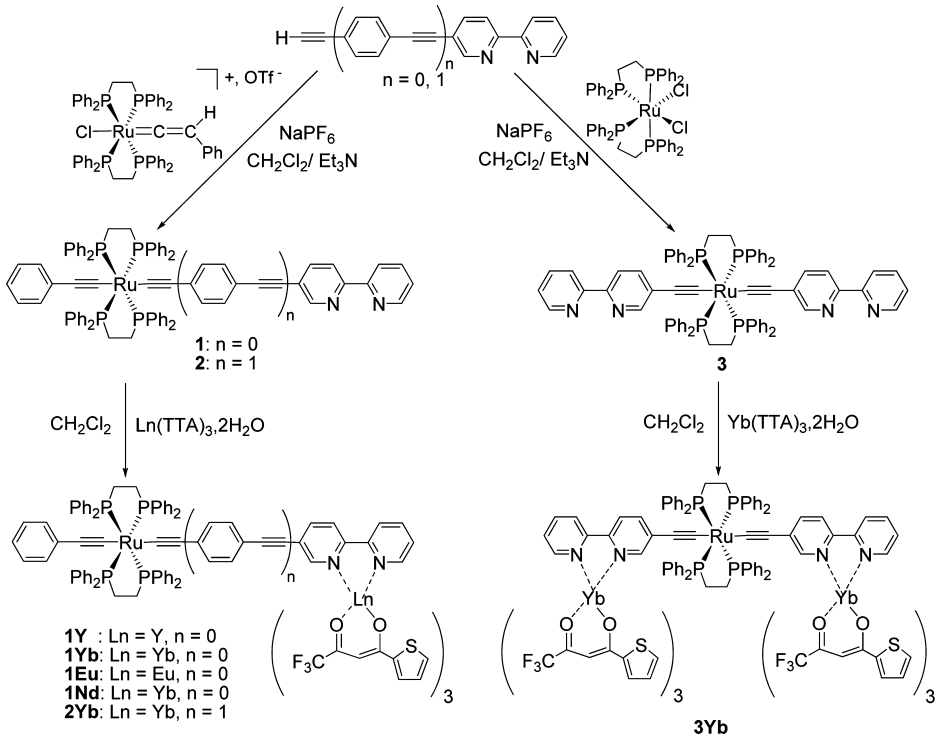

Scheme 2. Synthetic Pathway for [4Yb]OTf

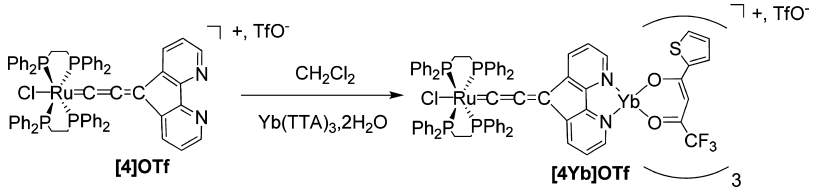

the redox commutation of the carbon-rich *antenna*, a concept that we recently extended to the redox control of single-molecule magnet properties for the Dy^{3+} ion.[16] Following these preliminary results, Faulkner,[17] Yano,[18] and Higushi[19] reported elegant modulations of Yb^{3+} or Eu^{3+} luminescence using a ferrocene redox-active antenna or triarylamine and Fe(bis-terpyridine) as redox-switchable quenching units.

Herein, we fully describe our work exploring the possibility of triggering through oxidation the luminescence properties of lanthanide complexes (Yb^{3+}, Nd^{3+}, Eu^{3+} , and Y^{3+}) featuring various redox-active carbon-rich ruthenium bipyridyl complexes as switchable antenna ligands. In addition to the initial antenna **1** (Scheme 1), we wanted to study two variations of this structure, i.e. with **2** and **3**, to improve the stability of the oxidized form. Indeed, these last two compounds presented an extended conjugated skeleton with a longer carbon-rich chain in **2** or with a symmetrical distribution with two equivalent carbon-rich chains in **3** and were designed with one parameter in mind: the "dilution" of the spin density on more atoms of the carbon-rich ligands in order to improve the stability of the oxidized lanthanide complexes. Finally, the allenylidene complex **4**[OTf] (Scheme 2) was also designed with the aim of observing the switching phenomenon on a cationic complex upon reduction.[20] Therefore, in this article we describe the synthesis and characterization of these new complexes, including the crystallographic structures of intermediates **1** and **3** and heterobimetallic complexes **1Nd** and **1Eu**. The electrochemical behaviors of all derivatives were investigated by cyclic voltammetry, and finally the optical and vibrational spectroscopic properties of the heterobimetallic complexes were thoroughly studied (absorption, emission, sensitization, and redox modulation of the luminescence) using a combination of electrochemical and spectroscopic techniques (UV/vis/NIR/IR), including Nd luminescence redox modulation for the first time.

RESULTS AND DISCUSSION

Synthesis of the Heteronuclear Complexes. The complexes were prepared as shown in Schemes 1 and 2. First, following a classical procedure,[21] combinations of HC≡C−bipy[22] or of HC≡C−C_6H_4−C≡C−bipy[23] with the well-known vinylidene precursor *trans*-[ClRu(dppe)$_2$=C=CHPh][OTf], in the presence of a noncoordinating salt ($NaPF_6$) and a base (Et_3N), led to the adducts **1** and **2**, bearing one bipyridine function, in good yield (77% and 76%, respectively). The synthesis of the bifunctional compound **3** was achieved in 75% yield by activation of H−C≡C−bipy with *cis*-[(dppe)$_2$$RuCl_2$] under identical conditions. Interestingly, this protocol gives the desired trans complex without scrambling products, in contrast to previous observations.[24] These three species were characterized by means of ^{31}P, ^{1}H, and ^{13}C NMR and IR spectroscopy and mass spectrometry.[25] As characteristic features, we observed the expected $\nu_{C\equiv C}$ vibration stretch for the acetylide complexes

dx.doi.org/10.1021/om500059d | *Organometallics* 2014, 33, 4824−4835

at ca. 2060 cm^{-1} in the FTIR spectra, a single resonance peak in the ^{31}P NMR spectra for a trans arrangement on the ruthenium atom in the typical region for bis(σ-arylacetylide) at ca. δ 52−55 ppm, and the characteristic resonances of the H_6 protons of noncoordinated bipyridine units in the ^1H NMR spectra at δ ~7.68 ppm. A further combination of equimolar quantities of [$Ln(TTA)_3{\cdot}2H_2O$] (Ln = Eu, Yb, Nd, Y) and of bipyridyl complex **1**, **2**, or **3** in dichloromethane led to the precipitation of the desired heterobimetallic (**1Eu**, **1Y**, **1Yb**, **1Nd**, **2Yb**) and heterotrimetallic complexes (**3Yb**). In parallel, combination of [$Yb(TTA)_3{\cdot}2H_2O$] with the allenylidene *trans*-[$Ru(dppe)_2Cl$-($C{=}C{=}C_{11}H_6N_2$)]OTf ([**4**]OTf), bearing a 4,5-diazafluorene functional group,[26] also led to the expected bimetallic derivative [**4Yb**]OTf. The FTIR measurements show for the five acetylide adducts a consistent shift of the $\nu_{C\equiv C}$ vibration stretch to lower energy for the heavier substituent, i.e. to 2030−2040 cm^{-1}, and the carbonyl vibration stretches for the TTA ligands at ca. 1600 and 1630 cm^{-1}. The structures of these new compounds were confirmed with the help of ^{31}P NMR and ^1H NMR spectroscopy, elemental analysis, and HR-MS.[27] In a dichloromethane solution, the ^1H NMR spectrum of the diamagnetic complex **1Y** shows only one set of signals at room temperature, in agreement with an overall 3-fold solution structure of the TTA ligands around the metal center.[28] A clear shift of the bipyridine protons is observed in comparison with those of the free ligand **1**, with for example a deshielding of the H_6 and $H_{6'}$ protons by 0.77 and 0.52 ppm, respectively.[29] The "$Ru(dppe)_2$" moiety is affected to a smaller extent with a ^{31}P NMR signal at 52.8 ppm (−0.3 ppm in comparison to that of **1**). For the lanthanide complexes, additional paramagnetic shifts are observed due to the through-space interactions between the observed nuclei and the 4f unpaired electrons (pseudocontact shifts) which depends on the magnetic anisotropy of the lanthanide ion (and on the spatial location of the nuclei with respect to its anisotropy tensor). We observed for **1Ln** a negative paramagnetic shift on the 6,6′-bipyridine protons for Ln = Nd and a positive shift for Ln = Eu, Yb (Figure 1). Paramagnetic shifts of opposite signs are seen for the methine proton of TTA (δ 6.22 for **1Y**, 11.33 for **1Nd**, 2.93 for **1Eu**, and −11.92 ppm for **1Yb**).[30,31] For [**4Yb**]OTf, the impact of Yb coordination on the chemical shifts of the organometallic moiety is much more important than for **1Yb**. The ^{31}P NMR signal is deshielded by 4.4 ppm in [**4Yb**]OTf in comparison to that of [**4**]OTf. In a similar way, the ^1H NMR signals from the dppe ligand are very deshielded with, for example, the *o*-phenyl proton signals at 13.44 and 11.59 ppm (7.17 and 6.97 ppm in [**4**]OTf) or the CH_2−P signals at 7.86 and 6.68 ppm (3.30 and 3.20 ppm in [**4**]OTf). Finally, line broadening and paramagnetic shifts of the azafluorene moiety are also more important for [**4**]OTf. These differences may result from a different orientation of the anisotropy tensor of the Yb ion in comparison to that of the Ru(dppe) fragment in the allenylidene and acetylide complexes, since the Ru−Ln distance should be rather similar in both types of complexes.

Crystallographic Studies. Good-quality crystals suitable for X-ray structure determinations were obtained from a dichloromethane/*n*-pentane biphasic mixture (2/1) with compounds **1** and **3**. Complexes **1Nd** and **1Eu** were crystallized by slow evaporation of dichloromethane/hexane (1/1) mixtures. The crystallographic data are given in Table 1. Labeled views of these structures, excluding solvent molecules, with selected bond lengths for all complexes are reported in Figures 2−5. The solvated complexes **1** and **3** crystallized in the monoclinic *C*2/*c* and triclinic $P\bar{1}$ space groups, respectively. The bond lengths and

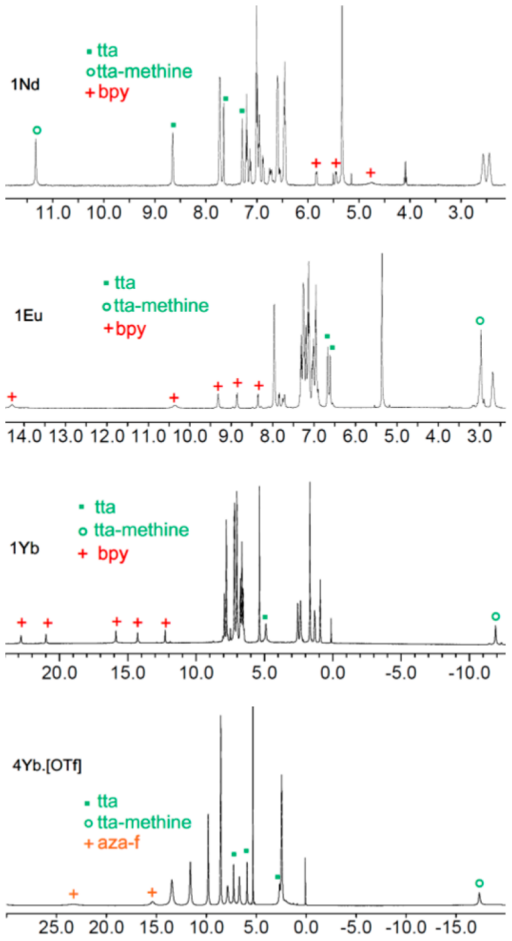

Figure 1. ^1H NMR spectra in CH_2Cl_2 of **1Nd**, **1Eu**, **1Yb**, and [**4Yb**]OTf.

angles of these complexes are not unusual in comparison with available X-ray data for related mononuclear bis-dppe Ru(II) acetylide complexes, including the distorted-transoid conformation of the bipyridyl moieties in the solid state, and warrant no further comments.[32,36,24] It is worth noting that the bipyridyl units are not hindered at all by the dppe ligand to tolerate further coordination (Figures 2 and 3).

The bimetallic complexes **1Nd** and **1Eu** are both isostructural with their latest rare-earth analogues **1Dy** ($P\bar{1}$ space group).[16] It is therefore reasonable to assume that isostructurality is also valid for **1Yb**, although its structure could not be determined. The structure of **1Nd**, depicted in Figures 4 and 5, is representative of both **1Nd** and **1Eu**. As expected, the organometallic moiety bond lengths and angles are only slightly affected by coordination. The lanthanide ion is eight-coordinated with a D_{4d} symmetry corresponding to a slightly distorted square antiprismatic coordination polyhedron (Figure 5). The two almost flat faces are (N72, N61, O10, O30) and (O7, O27, O47, O50) with respective bending angles of 6.30 and 2.02° (**1Eu**) and 6.72° and 1.38° (**1Nd**). The Ln−N distances are longer than the Ln−O distances (Table 2), and both are reduced when going from Nd to the smaller Eu and Dy ions.[16] The contraction along the lanthanide series has an effect on the distortion of the square-antiprismatic coordination sphere, which is more pronounced for the larger ions. This is confirmed by continuous shape measures (CSM)[33] performed with SHAPE 2.1,[34] which gives parameters of 0.743 for **1Nd**, 0.601 for **1Eu**, and 0.567 for **1Dy**, the ideal square antiprism being characterized by a value of 0. In the crystal

dx.doi.org/10.1021/om500059d | *Organometallics* 2014, 33, 4824−4835

Table 1. Crystal Data and Structure Refinement Parameters for 1, 3, 1Eu, and 1Nd

	1	3	1Eu	1Nd
formula	$(C_{72}H_{60}N_2P_4Ru)_2{\cdot}3CH_2Cl_2$	$C_{76}H_{62}N_4P_4Ru{\cdot}2CH_2Cl_2$	$C_{96}H_{72}EuF_9N_2O_6P_4RuS_3{\cdot}CH_2Cl_2$	$C_{96}H_{72}NdF_9N_2O_6P_4RuS_3{\cdot}CH_2Cl_2$
fw	2611.12	1426.1	2078.57	2070.85
cryst syst	monoclinic	triclinic	triclinic	triclinic
space group	$C2/c$	$P\bar{1}$	$P\bar{1}$	$P\bar{1}$
a (Å)	34.983(3)	9.3922(6)	13.032(5)	13.028(4)
b (Å)	14.0674(12)	13.4491(9)	18.320(10)	18.443(5)
c (Å)	24.973(2)	13.4491(9)	21.732(11)	21.825(6)
α (deg)	90	95.889(3)	66.60(2)	66.428(10)
β (deg)	94.000(5)	108.422(3)	73.40(2)	72.705(11)
γ (deg)	90	96.071(3)	77.08(2)	76.854(10)
V (Å^3)	12259.8(18)	1643.56(19)	4527(4)	4554(2)
Z	4	1	2	2
D_{ca} (g cm^{-3})	1.415	1.441	1.53	1.51
T (K)	100(2)	100(2)	150(2)	150(2)
final R	0.0657	0.0368	0.0865	0.0478
R_w	0.1769	0.096	0.1748	0.101

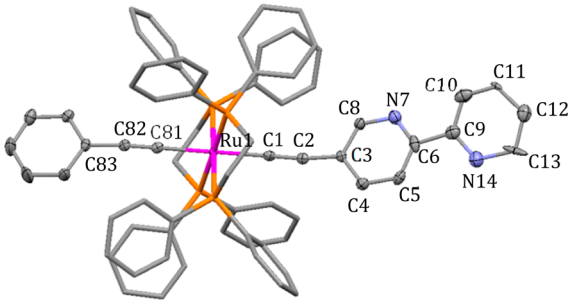

Figure 2. Simplified view of the crystal structure of **1** (H atoms omitted; dppe ligands plotted in wire style). Selected distances (Å) and angles (deg): Ru1−C1 2.062(4), Ru1−C81 2.067(4), C1−C2 1.223(6), C2−C3 1.434(6), C81−C82 1.210(6), C82−C83 1.438(6); C1−Ru1−C81 179.46(16), C2−C1−Ru1 175.2(3), C82−C81−Ru1 174.8(3), C1−C2−C3 172.0(5), C81−C82−C83 175.2(5), N7−C6−C9-C10 15.5(6).

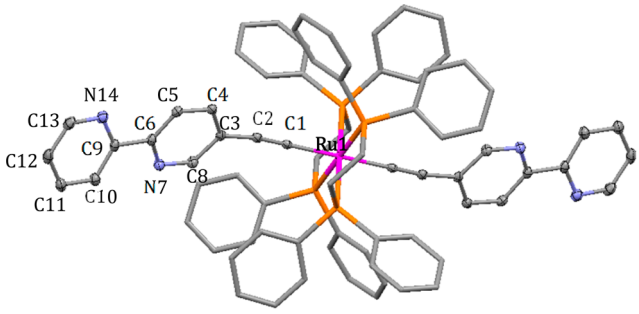

Figure 3. Simplified view of the crystal structure of **3** (H atoms omitted; dppe ligands plotted in wire style). Selected distances (Å) and angles (deg): Ru1−C1 2.061(2), C1−C2 1.218(3), C2−C3 1.430(3); C1−Ru1−C1^i 180.00(7), C2−C1−Ru1 175.22(17), C1−C2−C3 172.1(2), N7−C6−C9−C10 14.6(3).

packing, the complexes are paired via π stacking between their bipyridyl moieties with an interplane separation between the bipyridine mean planes of 3.41 Å.

Electrochemical Studies. Cyclic voltammetry (CV) was used to study the electrochemical behavior of all complexes (CH_2Cl_2, 0.2 M Bu_4NPF_6). All metal acetylides display a reversible one-electron oxidation followed by an irreversible process consistent with an undergoing chemical reaction of the

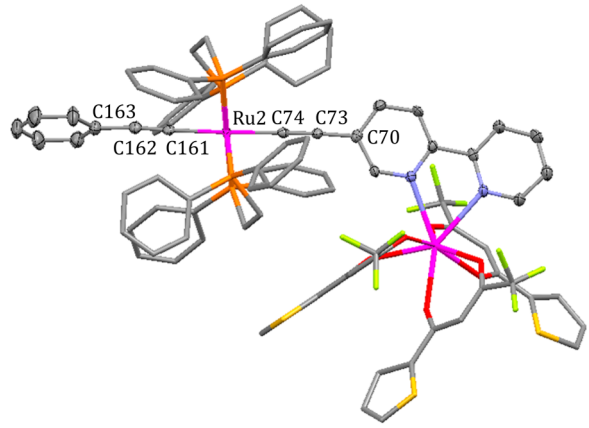

Figure 4. Simplified view of the crystal structure of **1Nd** (H atoms omitted, dppe and TTA ligands plotted in wire style). Selected distances (Å) and angles (deg) for **1Nd**: Ru2−C74 2.043(3), Ru2−C161 2.087(4), C74−C73 1.216(5), C73−C70 1.438(5), C161−C162 1.199(5), C162−C163 1.455(5); C161−Ru2−C74 178.07(13), C73−C74−Ru2 178.4(3), C162−C161−Ru2 176.9(3), C74−C73−C70 174.5(4), C161−C162−C163 174.7(4). Selected distances (Å) and angles (deg) for **1Eu**: Ru2−C74 2.049(10), Ru2−C161 2.082(10), C74−C73 1.208(13), C73−C70 1.459(13), C161−C162 1.205(14), C162−C163 1.438(16); C161−Ru2−C74 178.4(3), C73−C74−Ru2 178.9(8), C162−C161−Ru2 177.9(9), C74−C73−C70 173.3(10), C161−C162−C163 177.6(12).

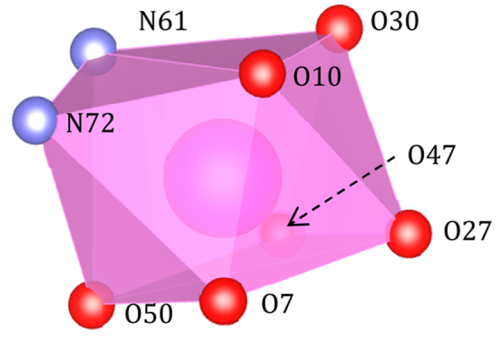

Figure 5. Coordination polyhedron of the neodynium center in **1Nd**.

second oxidized species. The values of the potentials are reported in Table 3, and a typical CV trace for the reversible process is

dx.doi.org/10.1021/om500059d | *Organometallics* 2014, 33, 4824−4835

Table 2. Bond Distances (Å) in the Lanthanide Coordination Spheres of 1Eu and 1Nd

	1Eu	1Nd
Ln−O47	2.342(8)	2.390(3)
Ln−O27	2.349(7)	2.411(3)
Ln−O50	2.398(7)	2.417(3)
Ln−O7	2.370(7)	2.405(2)
Ln−O30	2.371(6)	2.411(3)
Ln−O10	2.382(8)	2.434(3)
Ln−N61	2.577(8)	2.613(3)
Ln−N72	2.569(8)	2.608(3)

shown in Figure 6 for **1Eu**. The first oxidation process is often erroneously viewed as essentially involving the Ru^{III}/Ru^{II} couple, whereas it actually strongly involves the carbon-rich ligands.[3,35,36] For the allenylidene [**4Yb**]OTf, one reduction event is observed and is ascribed to the reduction of the cumulenic carbon chain.[20,26] Therefore, two points are worth noting: (i) the oxidation (reduction) potentials of acetylide (allenylidene) lanthanide complexes are consistently higher than those of the parent complexes owing to the electron-withdrawing character of the $Ln(TTA)_3$ moieties and (ii) lengthening of the bridge decreases the influence of the Ln coordination on the redox potential in **2Yb**. This is a token of a large contribution of the carbon-rich bridging ligands to the frontier orbitals of the complexes.

Optical Properties. The optical properties of all complexes were studied in CH_2Cl_2 solutions (Table 3). The acetylide heterometallic complexes show two main absorption bands above 300 nm at λ_{max} ~334 and ~460 nm (Table 3). As represented in Figure 7, the first transition is assigned to the TTA ligand absorption by comparison with $[Ln(TTA)_3{\cdot}2H_2O]$ precursors, probably overlapping with transitions of $\pi-\pi^*$ character centered on the bipyridyl moieties by comparison with their precursors **1**−**3**. On the other hand, the lower energy transition is characteristic of the ruthenium acetylide moiety, usually described as multiconfigurational metal-to-ligand charge transfer (MLCT) excitations corresponding to transitions from Ru(dπ)/alkynyl-based orbitals to metal/ligand antibonding orbitals combined with intraligand $\pi \rightarrow \pi^*$ character.[35,36] However, on the basis of preliminary DFT calculations,[37] it occurs that herein this transition might be the result of a charge

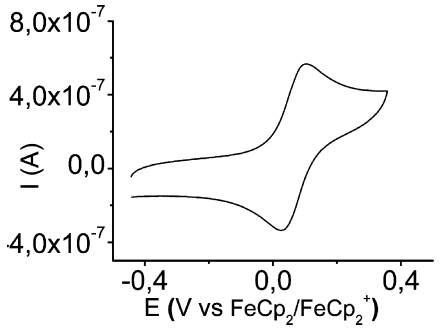

Figure 6. CV trace of **1Eu** (CH_2Cl_2, 0.2 M Bu_4NPF_6, ν = 100 mV s^{-1}).

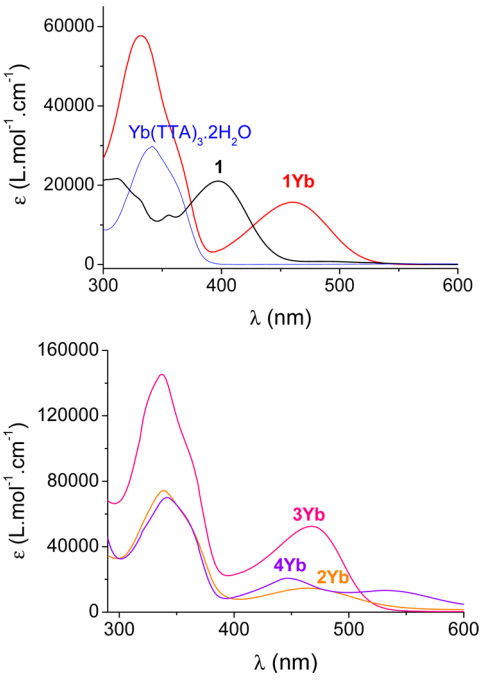

Figure 7. (top) Absorption spectra of **1** (black), $[Yb(TTA)_3{\cdot}2H_2O]$ (blue), and **1Yb** (red) in CH_2Cl_2. (bottom) Absorption spectra of **2Yb** (orange), **3Yb** (pink), and [**4Yb**]OTf (purple) in CH_2Cl_2.

Table 3. Electrochemical and Optical Data

	electrochemistry[a,b] $E°$/V				
	$E°(+/0)$	$E°(0/+)$	$E°(+/2+)$	UV−vis[e] λ_{max}/nm (ε/mol^{-1} L cm^{-1})	UV−vis[f] of oxidized species (NIR range) λ_{max}/nm (ε/mol^{-1} L cm^{-1})
1		−0.009	0.854[c]	308 (21600), 398 (21000)	
2		−0.015	0.824[c]	323 (27900), 422 (21150)	
3		0.078	0.963	272 (24400, sh), 406 (31000)	
[**4**]OTf[h]	−0.580			274 (59900), 453 (15700), 521 (13700)	
1Y		0.066	0.930[c]	334 (77100), 459 (20400)	1055 (8500)
1Yb		0.059	0.921[c]	334 (50100), 460 (15700)	1057 (5750)
1Eu		0.065	0.927[c]	334 (78600), 460 (16700)	1052 (7700)
1Nd		0.056	0.905[c]	336 (76000), 460 (15800)	1057 (5200)
2Yb		−0.002	0.860[c]	335 (74100), 469 (14450)	1170 (6910)
3Yb		0.162[d]	0.710[c]	335 (142000), 469 (51900)	1080 (20800)
[**4Yb**]OTf	−0.520[e]			335 (68180), 447 (20620), 532 (13170)	680 (10700)[g]

[a]Conditions: sample 1 mM, Bu_4NPF_6 (0.2 M) in CH_2Cl_2, ν = 100 mV·s^{-1}. Potentials are reported in V vs $FeCp_2/FeCp_2^+$ as an internal standard. [b]Reversible oxidation processes, $\Delta E_p \approx 60-70$ mV. [c]Peak potential of an irreversible process. [d]ΔE_p = 90 mV. [e]ΔE_p = 130 mV. [f]In CH_2Cl_2. [g]Upon a reduction process. [h]From ref 26.

dx.doi.org/10.1021/om500059d | *Organometallics* 2014, 33, 4824−4835

transfer from Ru(dπ)/alkynyl-based orbitals to a π^* orbital based on the bipyridine unit. This assignment is enforced by the marked bathochromic shift observed upon complexation of the parent ligand **1**−**3** to the lanthanide(III) ion ($\Delta\lambda_{max}$ = 47−62 nm). Indeed, such red shifts are characteristic of CT type transitions and are due to the enhancement of bipyridyl moiety electron-withdrawing character upon further complexation.[30,38] In the case of complexes **1Ln** and **3Yb**, the absorption spectra do not show the presence of the band at ca. 400 nm characteristic of uncomplexed ligand **1** or **3**, which unambiguously indicates that no dissociation occurs under dilute conditions (10^{-5}−10^{-6} mol L^{-1}).[30] For complex **2Yb** a concentration of at least 10^{-4} mol L^{-1} is needed to obtain concentration-independent absorption spectra. Below this value, the presence of uncomplexed compound **2** is observed owing to partial dissociation of **2Yb**. It is also worth noting that the wavelength of the maximum absorption does not depend on the identity of the central lanthanide ion in **1Ln** (Table 3), which is in agreement with previous literature results.[39] For the allenylidene [**4Yb**]OTf, the two transitions displaying the MLCT ($Ru^{II}(d\pi) \rightarrow \pi^*$-(allenylidene) at higher energy) and diazafluorene (lower energy) characters[26] are weakly affected upon complexation with the ytterbium ion.

The emission properties were first studied for the complex **1Y**, where no energy transfer can occur. Upon excitation in the lower energy transition (CT character), a broad, weak emission is observed around 675 nm (Figure 8). The nature of the emitting

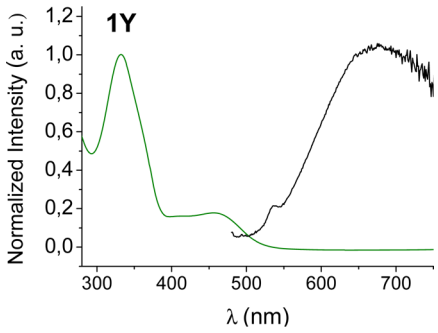

Figure 8. Absorption and emission spectra of **1Y** (λ_{ex} 450 nm) at room temperature in CH_2Cl_2.

state was not unambiguously determined. Nevertheless, whatever the sensitization process (singlet or triplet mediated)[13] this excited state appeared to be too low in energy to sensitize efficiently the Eu(III) luminescence.

In contrast, in the case of NIR emitting lanthanide ions, excitation in the aforementioned lower energy transition (λ_{ex} 450 nm) results in a very weak ligand-centered emission around 675 nm accompanied by a new characteristic line shape emission profile of Nd(III) ($^4F_{3/2} \rightarrow {}^4I_{9/2}$) at 898 nm ($^4F_{3/2} \rightarrow {}^4I_{9/2}$), 1063 nm ($^4F_{3/2} \rightarrow {}^4I_{11/2}$), and 1333 nm ($^4F_{3/2} \rightarrow {}^4I_{13/2}$) and of Yb(III) at 979 nm ($^2F_{5/2} \rightarrow {}^2F_{7/2}$) in the NIR spectral range (Figure 9). This indicates that a straightforward sensitization mechanism (vide infra) occurs from the Ru−acetylide ligand to the lanthanide ion, as [$Ln(TTA)_3{\cdot}2H_2O$] precursors do not absorb in that region. At room temperature, the Yb(III) luminescence decay of **1Yb** and **3Yb** can be nicely fitted by a monoexponential function, indicating the presence of a single species with excited state lifetimes of 10.3 and 10.6 μs, respectively. These values are in the classic range for this type of Yb(III) complex.[40] Note that, as expected, identical NIR emission spectra are obtained upon

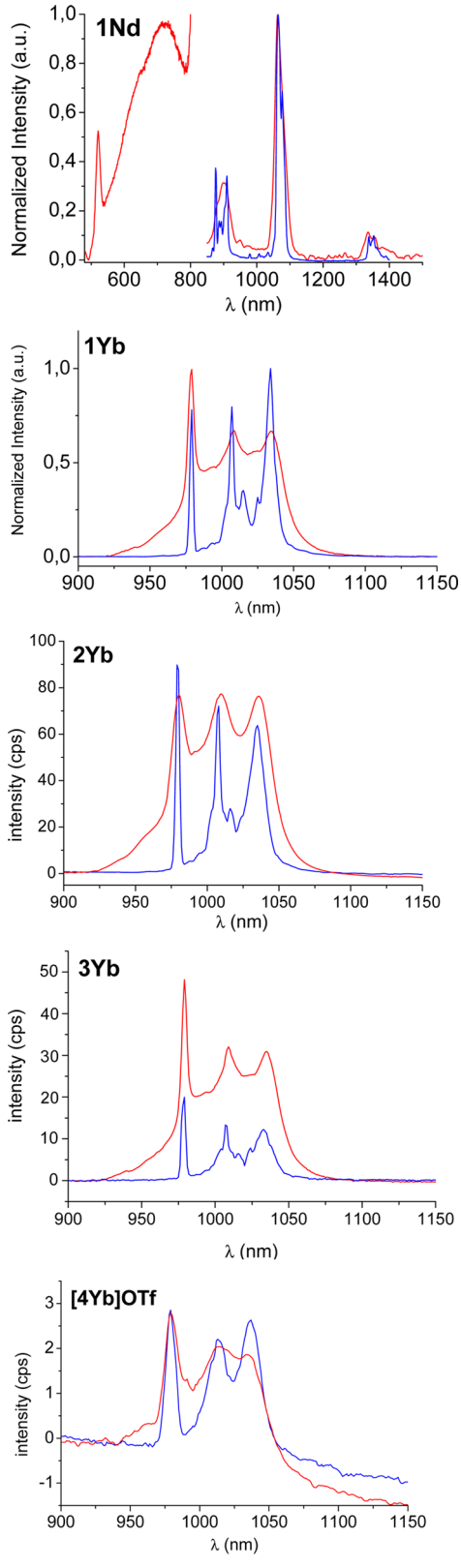

Figure 9. Emission spectra of **1Nd**, **1Yb**, **2Yb**, **3Yb**, and [**4Yb**]OTf (λ_{ex} = 450 nm) at room temperature in CH_2Cl_2 (red lines) and at 77 K in frozen organic glass (MeTHF for **1Ln**, CH_2Cl_2 for **2Yb**, **3Yb**, and [**4Yb**]OTf) (blue lines).

excitation in the TTA absorption band (λ_{exc} 360 nm). In contrast to the case for **1Yb**, the allenylidene compound **[4Yb]OTf** displays a very weak emission, suggesting that Ru−allenylidene

dx.doi.org/10.1021/om500059d | *Organometallics* 2014, 33, 4824−4835

moieties are less efficient antennas than the acetylide complexes (Figure 9).[41]

In a frozen organic solvents (MeTHF or CH_2Cl_2, 77 K) the vibronic broadening of the transitions is strongly reduced ($\omega_{1/2}$ = 27 cm^{-1}) and consequently the emission spectrum becomes nicely resolved and additional splitting of each transition, a signature of the ligand-field effect, is clearly observed. This splitting is particularly clear in the case of all ytterbium complexes, where four transitions can be identified that correspond to the degeneracy of the $^2F_{7/2}$ ground state. The total splittings of the ground state crystal field sublevels are estimated to be 544, 553, and 534 cm^{-1} for **1Yb**, **2Yb**, and **3Yb**, respectively, taking the most energetic transition as the origin. These values are typical for low-symmetry complexes and suggest that the structure of the complexes in solution is similar to that obtained by X-ray crystallography (distorted D_{4d} symmetry).[42]

Redox Behavior and Commutation of Luminescence. All of the heterometallic complexes present a reversible first oxidation/reduction process. Therefore, their absorption properties upon oxidation/reduction were investigated by means of UV/vis/NIR spectroelectrochemistry (SEC) in an optically transparent thin-layer electrochemical (OTTLE) cell. In the spectra of **1Y**, **1Eu**, **1Yb**, and **1Nd**, while the band located around 334 nm are barely affected upon one-electron oxidation, the intensity of the bands at λ_{max} ~450 nm decreases significantly. Meanwhile, a new broad absorption obviously including several transition bands is observed at low energy, in the NIR region of the spectrum at ca. 1055 nm (Table 3), the wavelength of the maximum absorption not being significantly dependent on the identity of the lanthanide ion. These broad bands are probably due to multiple transitions from HOMO-*n* to the SOMO resulting from the depopulation of the HOMO d_π/π orbital. While the bands involve some charge transfer from the metal groups to the carbon-rich ligand, they certainly exhibit a strong $\pi \rightarrow \pi^*$ (IL) character.[35] The other complexes, **2Yb** and **3Yb**, show a very similar behavior, and a representative example for all these complexes is depicted in Figure 10 with **3Yb**. Concerning the IR experiments conducted with the four acetylide complexes **1Y**, **1Eu**, **1Yb**, and **1Nd**, they display an expected shift of the $\nu_{C\equiv C}$ vibration stretch from 2043−2044 to 1907−1908 cm^{-1} upon electron removal (Figure 9b), due to the bond weakening of the acetylide linkages demonstrating a large involvement of the central bis(ethynyl) ruthenium moiety in the first oxidation process. As expected, the opposite shift is observed for [**4Yb**]OTf upon reduction with the move of the allenylidene vibration stretch from 1914 to 1977 cm^{-1} and the collapse of the former MLCT and diazafluorene bands with the appearance of a new band at 608 nm tentatively ascribed to the diazafluorene moiety. Note that all experiments were carried out under inert conditions with Schlenk techniques. The spectroelectrochemical experiments showed a reversibility of 90−100% on the basis of the absorption intensities recovered at the end of the experiments with no features other than those of the parent materials.

On the basis of the luminescence measurements, as the ruthenium carbon-rich unit is not an effective antenna for the Eu^{3+} ion and the luminescence of [**4Yb**]OTf is very weak, redox switching experiments were attempted on **1Yb**, **1Nd**, **2Yb**, and **3Yb**. Primarily, oxidation was probed chemically by successive addition of equimolar amounts of an oxidant (acetylferrocenium, E° = 0.270 V vs $FeCp_2/FeCp_2^+$) and of a reductant (decamethylferrocene, E° = −0.590 V vs $FeCp_2/FeCp_2^+$) in the fluorescence cell under an inert atmosphere. Absorption and

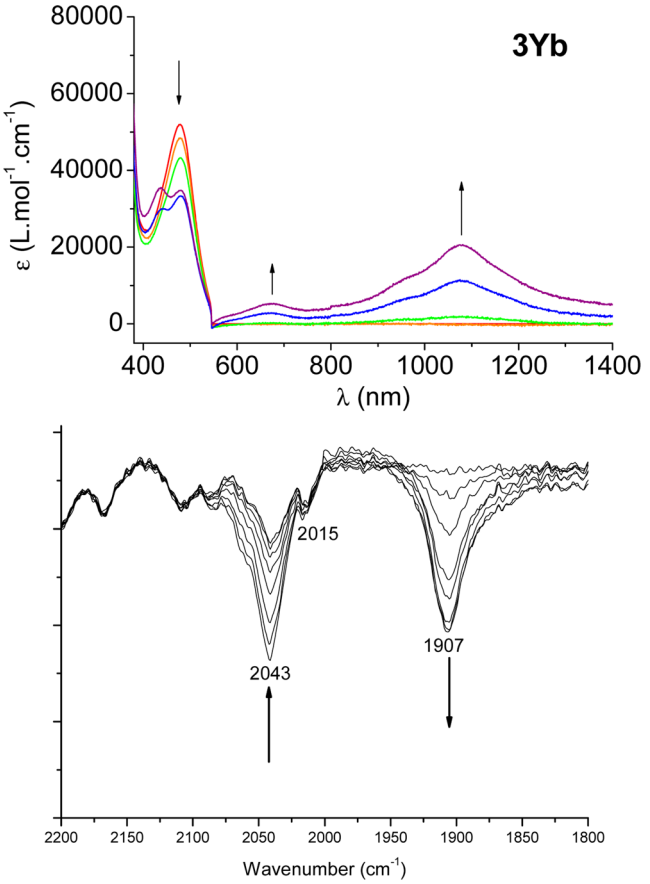

Figure 10. Spectroscopic changes (top) for **3Yb** in the UV/vis/NIR range and (bottom) for **1Yb** in the IR range during the first oxidation in 0.2 M NBu_4PF_6/1,2-$C_2H_4Cl_2$.

emission spectroscopy was used to monitor the evolution of the absorption and of the luminescence spectrum during these operations. Therefore, upon oxidation of all complexes, we observed the expected decrease of the absorption band at λ_{max} 430−469 nm along with the appearance of a new broad band around 1000−1200 nm, which is a clear signature of the formation of the oxidized forms in solution (vide supra). In the meantime, the nonemissive behavior of these oxidized forms is observed with the vanishing of the luminescence (Figure 11). A further chemical reduction process regenerated the neutral complexes, as underlined by the recovery of the luminescence for **1Yb**, **1Nd**, and **3Yb** of 53%, 31%, and 50% of their original intensities, respectively. In contrast to SEC experiments, the chemical redox switching is not fully reversible. Importantly, in all these luminescence modulation experiments, the absorption spectra also show a limited reversibility of the absorption intensity at λ_{max} 459−469 nm consistent with the emission experiments. This lack of full luminescence and absorption reversibility is attributed to the poor stability of the cationic species under the luminescence experimental conditions (high dilution: OD < 0.1, $C < 10^{-6}$ mol L^{-1}, addition of reactants), allowing the well-known hydrolysis of the acetylide ligand to a carbonyl adduct,[36,43] as a characteristic vibration stretch is observed at 1983 cm^{-1} via IR monitoring of the chemical switching experiment with **1Yb**.[15] Note that (i) owing to these dilution conditions, a clean experiment could not be obtained with **2Yb** (vide supra) and (ii) it seems that our strategy to

dx.doi.org/10.1021/om500059d | *Organometallics* 2014, 33, 4824−4835

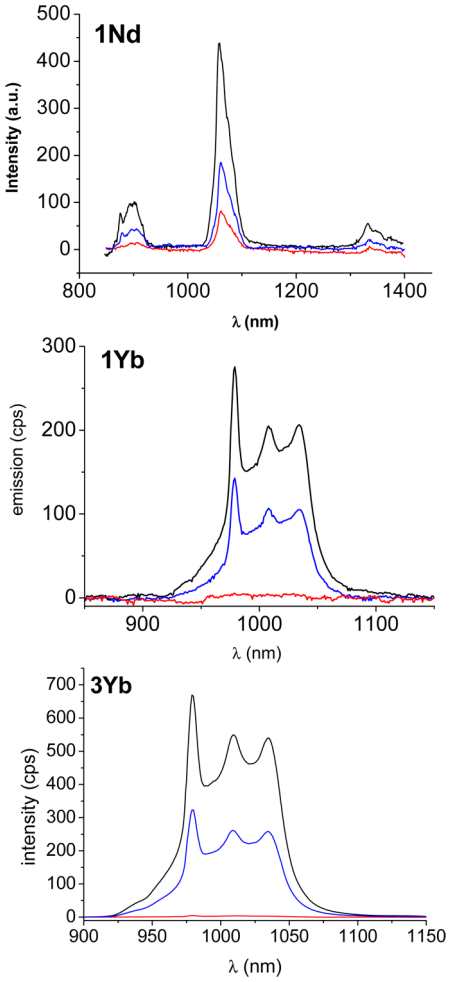

Figure 11. Monitoring of the emission spectra (λ_{ex} 450 nm) during the first oxidation of (top) **1Nd**, (middle) **1Yb**, and (bottom) **3Yb**: initial emission spectrum in CH_2Cl_2 (black), after in situ oxidation with acetylferrocenium (red), and after reduction with decamethylferrocene (blue).

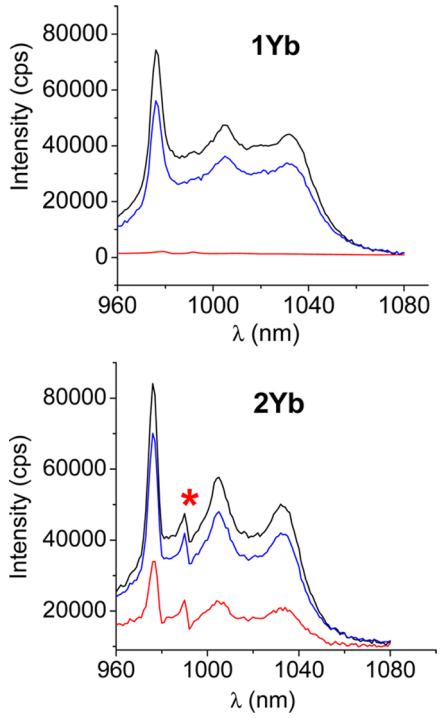

Figure 12. Monitoring of the emission spectra (λ_{ex} 440 nm) upon the first oxidation of **1Yb** (top) and **2Yb** (bottom) in an OTTLE cell (CH_2Cl_2, 0.2 M Bu_4NPF_6): initial emission spectrum in CH_2Cl_2 (black), after oxidation at 0.8 V vs Ag/Ag^+ (red), and after reduction at 0 V (blue). The asterisk shows a cell artifact.

increase stability with the antenna **3** did not lead to significant improvements.

Therefore, we also attempted to modulate the luminescence of complexes **1YB** and **2YB** electrochemically by using a 1 mm path length quartz electrochemical cell with a CH_2Cl_2 solution including 0.2 M NBu_4NPF_6 as the supporting electrolyte and a Pt-gauze working electrode. Figure 12 shows the luminescence response obtained for both complexes (λ_{ex} 440 nm). Upon oxidation at 0.8 V vs Ag/Ag^+, the emission intensity decreases of ca. 100 and 85% of its original value (quenching) in about 240 s for **1Yb** and **2Yb**, respectively. Further reduction of this solution at 0 V leads to the recovery of 87 and 85% of the original intensity, respectively. For comparison, under electrochemical conditions, Faulkner's group achieved ca. 40% quenching for Yb and Eu adducts with the Fc antenna, whereas Yano reached 90% quenching with Eu using a β-diketonate chromophore and an intramolecular triarylamine redox quencher. Therefore, as expected, this experiment performed in a more concentrated medium, similar to that used for UV/vis/NIR SEC experiments, without any perturbation due to addition of reactants leads to a significant improvement of the stability of the system. As this electrochemical cell is not optimized, this result also leaves room for further improvements of efficiency, time scale, and reversibility.

Sensitization of lanthanide ion luminescence usually occurs via energy transfer from the antenna ligand.[12] The extinction of NIR luminescence in the Nd^{3+} and Yb^{3+} complexes can thus be rationalized by the oxidation of the ruthenium acetylide moieties, which prevents any sensitization by the appearance of new excited states at ca. 1000−1200 nm. These new low-lying excited states can either prohibit the sensitization or afford a preferential nonradiative back energy transfer pathway from the Yb^{3+} or Nd^{3+} excited states. Note that Yb^{3+} sensitization can also proceed via electron transfer from the electroactive ligand.[44] Thus, the extinction of NIR luminescence in the oxidized ytterbium complexes can also be rationalized by the oxidation of the ruthenium acetylide moieties preventing any sensitization by the electron transfer mechanism, triggering ytterbium luminescence quenching.

CONCLUSION

In this work, we could build efficient low potential redox active antenna with carbon-rich ruthenium units for the sensitization of Nd^{3+} and Yb^{3+} NIR emitters. Sensitization of the Eu^{3+} ion was not efficient, probably owing to the low energy level of these antennas, in contrast to that of ferrocene. Their redox properties also allowed for low-potential redox modulation of NIR luminescence of the Yb^{3+} ion and, for the first time, of the Nd^{3+} ion. For this purpose, chemical and electrochemical modulations were achieved. The electrochemical experiment showed a significantly improved efficiency with respect to the chemical experiments and leaves room for further improvements. Importantly, this work demonstrates that, with a precise molecular engineering, selective electrical modulation of differ-

dx.doi.org/10.1021/om500059d | *Organometallics* 2014, 33, 4824−4835

ent lanthanide ion luminescence should be possible with accurate redox-active chromophores allowing selective switchable sensitizations. In addition, further functionalization of such systems offers an enhanced potential for increasing functionality and/or for introducing anchoring moieties for future integration in molecular devices.

EXPERIMENTAL SECTION

General Comments. The reactions were carried out under an inert atmosphere using Schlenk techniques. were dried and distilled under argon using standard procedures. ^{1}H, ^{13}C, and ^{31}P NMR spectra were recorded on a Bruker AC 250, Bruker Avance III 400, Bruker Avance III Kryo-Platform 600 MHz, or Varian Unity INOVA 400 spectrometer in $CDCl_3$ or CD_2Cl_2 solutions at 303 K. The assignment of ^{13}C NMR signals was aided by HSQC and HMBC experiments. Numbering of the dppe, TTA, and acetylide ligands used for NMR assignment of complexes is displayed on Scheme 3. HR-MS spectra were recorded on a

Scheme 3. Numbering of the dppe, TTA, and Acetylide Ligands Used for NMR Assignment of Complexes[a]

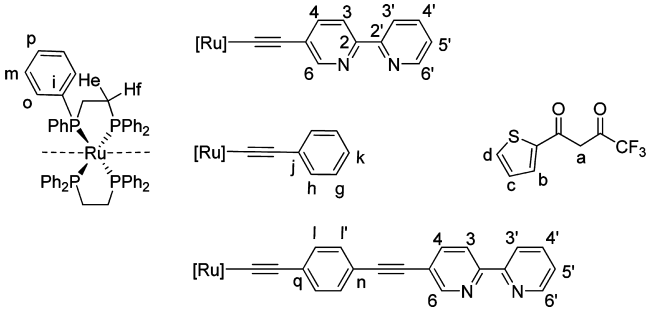

[a]For Nd, Yb, and Eu complexes, it was not possible to assign all of the signals precisely. On the basis of integration, it is possible to differentiate $H_T = H_b$, H_c, H_d, $H_B = H_3$, $H_{3'}$, H_4, $H_{4'}$, $H_{5'}$, H_6, $H_{6'}$, and the remaining signals.

Bruker MicrO-Tof-Q 2 spectrometer. Note that, for some paramagnetic lanthanide complexes, it was not possible to assign all of the signals precisely. X-ray measurements were performed at 100(2) K with a crystal mounted on a glass fiber on a Stoe IPDS II diffractometer (graphite monochromator, Mo Kα radiation, λ = 0.71073 Å). The ruthenium complexes *trans*-[Cl(dppe)$_2$Ru=C=CHPh][OTf],[45] *cis*-(dppe)$_2$RuCl$_2$,[46] ethynyl-2,2′-bipyridine,[22] HC≡C−C$_6$H$_4$−C≡C−bipy,[23] and *trans*-[Cl(dppe)$_2$Ru=C= C=C$_{11}$H$_6$−N$_2$][OTf][26] have been obtained as previously reported. $LnCl_3{\cdot}6H_2O$ was purchased from Aldrich (99.998%), and $Ln(TTA)_3{\cdot}2H_2O$ was prepared according to the literature.[47]

Electrochemical studies were carried out under argon using an Eco Chemie Autolab PGSTAT 30 potentiostat (CH_2Cl_2, 0.1 M Bu_4NPF_6); the working electrode was a Pt disk, and ferrocene was the internal reference.[48] In the case of **3Yb**, the solubility of the compound was too low to allow a CV measurement. Therefore, 2 equiv of $Yb(TTA)_3{\cdot}2H_2O$ was added to an electrolytic solution of **3** to generate **3Yb** in situ (as checked by an UV/vis absorption spectrum).

UV/vis/NIR spectroelectrochemistry (SEC) experiments were performed at 20 °C, under argon, with a homemade optically transparent thin-layer electrosynthetic (OTTLE) cell, path length 1 mm, using a Varian CARY 5000 spectrometer and an EG&G PAR Model 362 potentiostat. Pt mesh was used as the working electrode, Pt wire as the counter electrode, and Ag wire as a pseudoreference electrode. The electrodes were arranged in the cell such that the Pt mesh was in the optical path of the quartz cell. The anhydrous freeze−pump−thaw degassed sample−electrolyte solution (0.2 M *n*-Bu_4NPF_6) was cannula-transferred under argon into a cell that was previously thoroughly deoxygenated. Stable isobestic points were observed during oxidation or reduction. In every case rereduced or reoxidized samples displayed in the spectral region of interest no features other than those of the parent material. IR experiments were performed under similar conditions using a modified cell with KBr windows and a Bruker IFS28 spectrometer.

The luminescence spectra were measured using a Horiba-Jobin Yvon Fluorolog-3 spectrofluorimeter, equipped with a three-slit double grating excitation and emission monochromator with dispersions of 2.1 nm/mm (1200 grooves/mm). The steady-state luminescence was excited by unpolarized light from a 450 W xenon CW lamp and detected at an angle of 90° for dilute solution measurements by a red-sensitive Hamamatsu R928 photomultiplier tube. Spectra were reference corrected for both the excitation source light intensity variation (lamp and grating) and the emission spectral response (detector and grating). Uncorrected near-infrared spectra were recorded at an angle of 90° using a liquid nitrogen cooled, solid indium/gallium/arsenic detector (850−1600 nm) through a RG830 2 mm filter. The chemical oxidation−reduction experiments were carried out under a rigorously inert atmosphere directly in the luminescence cuvette using a homemade cell with Schlenk techniques. To that end, we used a homemade luminescence cell equipped with a Young valve and a connection to a vacuum line. The excitation of the Yb(III) luminescence decays was performed with an optical parametric oscillator from Ekspla, pumped with a pulsed frequency tripled YAG:Nd laser. The pulse duration was 6 ns at a 10 Hz repetition rate. The detection was ensured by a R1767 Hamamatsu photomultiplier through a Jobin-Yvon monochromator equipped with a 1 μm blazed grating. The signal was visualized and averaged with a Lecroy digital oscilloscope. Emission spectroelectrochemistry (SEC) experiments were performed at 20 °C, under argon, with a homemade OTTLE cell, path length 1 mm, using an FLSP920 spectrometer (Edinburgh Instruments) and an EG&G PAR Model 362 potentiostat. A Pt grid was used as the working electrode, a Pt wire as the counter electrode, and an Ag wire as a pseudoreference electrode. The cell was disposed with a 45° angle relative to the excitation beam provided by a CW 450 W xenon Arc Lamp. Near-infrared spectra were recorded at an angle of 90° using a liquid nitrogen cooled NIR PMT detector. Spectra were corrected from emission of the Pt grid.

***trans*-[PhC≡C−(dppe)$_2$Ru−C≡C−bipy] (1).** In a Schlenk tube, *trans*-[ClRu(dppe)$_2$=C=CHPh]$^+$(OTf)$^-$ (314 mg, 0.265 mmol), $NaPF_6$ (89 mg, 0.53 mmol), and 5-ethynyl-2,2′-bipyridine (60 mg, 0.33 mmol) were dried under vacuum for 30 min. Then, dichloromethane (25 mL) commixed with triethylamine (0.3 mL) was saturated with argon and transferred into the Schlenk tube. More triethylamine (0.2 mL) was then added. The mixture was stirred at room temperature for 40 h, and then the solution was filtered and taken to dryness under vacuum. The residue was redissolved in CH_2Cl_2 (40 mL), and the solution was washed with degassed water (5 × 10 mL) and dried (Na_2SO_4). Then, the solvent was evaporated, and the residue was washed with pentane (2 × 30 mL). Column chromatography on alumina (elution CH_2Cl_2/pentane 1/1) led to a yellow powder (240 mg, 0.204 mmol, 77%). ^1H NMR (500 MHz, $CDCl_3$, ppm): δ 8.67 (d, ^3J(H,H) = 4.0 Hz, 1H, H_6), 8.34 (d, ^3J(H,H) = 8.0 Hz, 1$H_{6'}$), 8.09 (m, 2H, $H_{3'}$ and H_3), 7.80 (td, ^3J(H,H) = 8 Hz and ^4J(H,H) = 1.5 Hz, 1H, $H_{4'}$), 7.70 (m, 8H, H_o), 7.38 (m, 8H, H_o), 7.30−6.86 (m, 31H, H_{ar}), 2.64 (s, 8H, H_e and H_f). ^1H NMR (300 MHz, CD_2Cl_2, ppm): δ 8.65 (d, ^3J(H,H) = 4.0 Hz, 1H, $H_{6'}$), 8.39 (d, ^3J(H,H) = 8.0 Hz, 1H, $H_{3'}$), 8.19 (d, ^3J(H,H) = 8.2 Hz, 1H, H_3), 8.02 (d, ^3J(H,H) = 1.5 Hz, 1H, H_6), 7.85 (m, 1H, $H_{4'}$), 7.44−6.98 (m, 46H, H_{ar}), 6.89 (d, ^3J(H,H) = 7.0 Hz, 2H, H_h), 2.70 (s, 8H, H_e and H_f). $^{13}C\{^1H\}$ NMR (75 MHz, CD_2Cl_2, ppm): δ 156.65 (s, $C_{2'}$), 150.27 (s, C_6), 149.32 (s, C_2), 149.02 (s, $C_{6'}$), 137.24 (s, C_4), 137.16 (m, C_i), 136.75 (m, C_i), 136.57 (s, $C_{4'}$), 134.36 (m, C_o), 133.97 (m, C_o), 130.45 (s, C_j)), 129.82 (s, C_h), 128.70 (s, C_p), 128.82 (s, C_p), 127.58 (s, C_g), 127.06 (s, C_m), 123.09 (s, C_k), 122.6 (s, $C_{5'}$), 120.23 (s, $C_{3'}$), 119.6 (s, C_3), 117.433 (s, −C≡C-C_6H_5), 113.58 (s, −C≡C-bipy), 31.4 (m, ^1J(P,C) + ^3J(P,C) = 24 Hz, P(CH_2)$_2$P). IR (KBr, cm^{-1}): 2057 ($\nu_{C\equiv C}$) (s). FAB$^+$-HRMS (m/z): [M + H]$^+$ 1179.2858 (calculated 1178.2829). Anal. Found for $[C_{72}H_{60}N_2RuP_4]{\cdot}1.33CH_2Cl_2$: C, 68.44; H, 4.88; N, 2.25. Calcd: C, 68.20; H, 4.89; N, 2.17.

***trans*-[Ph−C≡C−(dppe)$_2$Ru−C≡C−bipy-κ^2*N*,*N*′−Yb(TTA)$_3$] (1Yb).** In a Schlenk tube, $Yb(TTA)_3{\cdot}2H_2O$ (48.6 mg, 0.055 mmol) and

dx.doi.org/10.1021/om500059d | *Organometallics* 2014, 33, 4824−4835

trans-[Ru(dppe)$_2$(−C≡C-Ph)(−C≡C-bpy)] (**1**; 65.6 mg, 0.055 mmol) were dried under vacuum for 30 min and then dissolved in CH_2Cl_2 (30 mL). The solution was stirred at ambient temperature for 16 h. The mixture was taken to dryness under vacuum. The residue was washed with pentane (2 × 10 mL) and recrystallized from 1/2 CH_2Cl_2/pentane to yield poor-quality orange crystals (105 mg, 95%). ^{1}H NMR (500 MHz, CD_2Cl_2, ppm): δ 22.81 (s, 1H, H_B), 20.95 (s, 1H, H_B), 15.87 (s, 1H, H_B), 14.28 (s, 1H, H_B), 12.26 (s, 1H, H_B), 6.50−7.93 (m, 53H, H_B, H_T, H_{ar}), 4.89 (s, 3H, H_T), 2.56 (bs, 4H, H_e), 2.36 (br. s, 4H, H_f), −11.92 (br. s, 3H, H_a). ^{31}P NMR (400 MHz, CD_2Cl_2, ppm): 52.9. IR (KBr, cm^{-1}): 2043 (s) ($\nu_{C\equiv C}$), 1630 (s) and 1604 (s) ($\nu_{C=O}$), 1180 (s) (ν_{C-F}). FAB$^+$-HRMS (*m*/*z*): [M]$^+$ 2015.1829 (calculated 2015.1792). Anal. Found for [$C_{96}H_{72}F_9N_2O_6P_4RuS_3Yb$]·2$CH_2Cl_2$: C, 53.80; H, 3.44; N, 1.35; S, 4.55. Calcd: C, 53.88; H, 3.51; N, 1.28; S, 4.40. Solvent inclusion is consistent with crystal structures of **1** and of related compounds.[24]

***trans*-[Ph−C≡C−(dppe)$_2$Ru−C≡C−bipy-κ^2*N*,*N*′−Nd(TTA)$_3$] (1Nd).** The same procedure as that described above was used with 22.6 mg (0.027 mmol) of Nd(TTA)$_3$·2H_2O and 22.6 mg (0.0192 mmol) of *trans*-[Ru(dppe)$_2$(−C≡C−Ph)(−C≡C-bpy)] to afford 20.2 mg of **1Nd** (53%).[49] ^{1}H NMR (500 MHz, CD_2Cl_2, ppm): δ 11.33 (bs, 3H, H_a), 8.65 (bs, 3H, H_T), 7.73 (m, 8H, H_o), 7.64 (d, *J* = 4.5 Hz, 3H, H_T), 7.29 (m, 3H, H_T), 7.20 (m, 4H, H_p), 7.13 (t, 2H, *J* = 7.5 Hz, H_g), 7.00 (m, 9H, H_k and H_m), 6.95 (m, 4H, H_p), 6.88 (d, 2H, *J* = 7.5 Hz, H_h), 6.76−6.70 (m, 2H, H_4 and $H_{4'}$), 6.46 (m, 8H, H_m), 5.85 (d, 1H, *J* = 7.5 Hz, H_3 or $H_{3'}$), 5.47 (d, 1H, *J* = 7.5 Hz, H_3 or $H_{3'}$), 4.75 (bs, H_6 and $H_{6'}$), 2.56 (4H, H_e), 2.45 (4H, H_f). ^{31}P NMR (400 MHz, CD_2Cl_2, ppm): δ 52.5. UV−vis: λ_{max} 335 nm (ε = 76200 L mol^{-1} cm^{-1}) and 464 nm (ε = 15700 L mol^{-1} cm^{-1}). IR (KBr, cm^{-1}): 2042 ($\nu_{C\equiv C}$) (s), 1628 (m) and 1604 (vs) ($\nu_{C=O}$). ESI (+) HRMS (*m*/*z*): [M]$^+$ 1985.1507 and 1983.1523 (calculated 1985.15038 for ^{144}Nd and 1983.14802 for ^{142}Nd). Anal. Found: C, 54.57; H, 3.54; N, 1.41; S, 4.57. Calcd for [$C_{96}H_{72}N_2O_6F_9S_3P_4RuNd$]·2$CH_2Cl_2$: C, 54.60; H, 3.55; N, 1.30; S, 4.46.

***trans*-[Ph−C≡C−(dppe)$_2$Ru−C≡C−bipy-κ^2*N*,*N*′−Eu(TTA)$_3$] (1Eu).** The same procedure as that described above was used with 43.4 mg (0.051 mmol) of Eu(TTA)$_3$·2H_2O and 60 mg (0.051 mmol) of *trans*-[Ru(dppe)$_2$(−C≡C−Ph)(−C≡C−bpy)]. Purification was achieved by recrystallization from dichloromethane and pentane to afford 96.5 mg of **1Eu** (95%).[49] ^{1}H NMR (500 MHz, CD_2Cl_2, ppm): δ 14.3 (bs, 1H, H_6 or $H_{6'}$), 10.3 (bs, 1H, H_6 or $H_{6'}$), 9.27 (m, 1H, $H_{4'}$), 8.82 (d, *J* = 7.5 Hz, 1H, $H_{3'}$ or $H_{5'}$), 8.31 (d, *J* = 7.0 Hz, 1H, $H_{3'}$ or $H_{5'}$), 7.92 (m, 8H, H_o), 7.84 (d, *J* = 8.0 Hz, 1H, H_B), 7.70 (m, 2H, C_6H_5−C_2), 7.31 (m, 4H, H_p), 7.26 (m, 9H, H_o and H_B), 7.20−7.00 (3H, C_6H_5−C_2), 7.19 (d, *J* = 5.0 Hz, 3H, H_T), 7.13 (m, 8H, H_m), 7.01 (m, 4H, H_p), 6.95 (m, 8H, H_m), 6.63 (bs, 3H, H_T), 6.57 (bs, 3H, H_T), 2.93 (s, 3H, H_a), 2.94 (4H, H_e), 2.64 (4H, H_f). ^{31}P NMR (400 MHz, CD_2Cl_2, ppm): δ 52.7. UV−vis: λ_{max} 336 nm (ε = 78600 L mol^{-1} cm^{-1}) and 462 nm (ε = 16800 L mol^{-1} cm^{-1}). IR (KBr, cm^{-1}): 2043 ($\nu_{C\equiv C}$) (s), 1626 (m) and 1601 (vs) ($\nu_{C=O}$). ESI-HRMS (*m*/*z*): [M]$^+$ 1994.1637 (calculated 1994.16153). Anal. Found: C, 53.87; H, 3.49; N, 1.27 . Calcd for [$C_{96}H_{72}N_2O_6F_9P_4S_3RuEu$]·2$CH_2Cl_2$: C, 54.45; H, 3.45; N, 1.30.

***trans*-[Ph−C≡C−(dppe)$_2$Ru−C≡C−bipy-κ^2*N*,*N*′−Y(TTA)$_3$] (1Y).** The same procedure as that described above was used with 44.2 mg (0.056 mmol) of Y(TTA)$_3$·2H_2O and 40 mg (0.034 mmol) of *trans*-[Ru(dppe)$_2$(−C≡C−Ph)(−C≡C−bpy)] to afford 29 mg of **1Y** (44%). ^{1}H NMR (500 MHz, CD_2Cl_2, ppm): δ 9.16 (d, *J* = 4.5 Hz, 1H, $H_{6'}$), 8.80 (s, 1H, H_6), 7.95 (m, 2H, H_B), 7.80 (m, 8H, H_o), 7.68 (t, 2H, *J* = 7.5 Hz, H_g), 7.56 (d, *J* = 4.5 Hz 3H, H_d), 7.43 (d, *J* = 5.0 Hz, 3H, H_b), 7.39 (m, 2H, H_B), 7.23 (m, 4H, H_p), 7.16 (m, 3H, H_c), 7.06−6.95 (m, 25H, C_6H_5−C_2, H_B and dppe), 6.78 (m, 8H, H_m), 6.34 (d, 1H, *J* = 7.0 Hz, H_B), 6.22 (s, 3H, H_a), 2.77 (4H, H_e), 2.55 (4H, H_f). ^{31}P NMR (400 MHz, CD_2Cl_2, ppm): δ 52.8. UV−vis: λ_{max} 331 nm (ε = 77100 L mol^{-1} cm^{-1}) and 459 nm (ε = 20500 L mol^{-1} cm^{-1}). IR (KBr, cm^{-1}): 2044 ($\nu_{C\equiv C}$) (s), 1623 (m) and 1604 (vs) ($\nu_{C=O}$). ESI-HRMS (*m*/*z*): [M]$^+$ 1930.1473 (calculated 1930.14614). Anal. Found: C, 54.21; H, 3.47; N, 1.24; S, 4.13. Calcd for [$C_{96}H_{72}N_2O_6F_9P_4S_3RuY$]·3$CH_2Cl_2$: C, 54.41; H, 3.60; N, 1.28; S, 4.40.

***trans*-[Ph−C≡C−(dppe)$_2$Ru−C≡C−C$_6$H$_4$−C≡C−bipy] (2).** In a Schlenk tube, *trans*-[ClRu(dppe)$_2$=C=CH-Ph]$^+$(OTf)$^-$ (200 mg, 0.169 mmol), $NaPF_6$ (57 mg, 0.338 mmol), and HC≡C−C_6H_4−C≡C−bipy (49,7 mg, 0.177 mmol) were dried under vacuum for 30 min. Then, dichloromethane (15 mL) commixed with triethylamine (1.5 mL) was saturated with argon and transferred into the Schlenk tube. The mixture was stirred at room temperature for 40 h, and 10 mL of methanol was added to induce the precipitation of the product. The residue was washed with methanol (3 × 10 mL) and pentane (2 × 10 mL) and dried to obtain a yellow powder (165 mg, 0.129 mmol, 76%). ^{1}H NMR (400 MHz, CD_2Cl_2, ppm): δ 8.80 (s, 1H, H_6), 8.69 (d, ^3J(H,H) = 4.8 Hz, 1H, $H_{6'}$), 8.46 (m, 2H, H_3 and $H_{3'}$), 7.95 (dd, ^3J(H,H) = 8.3 Hz and ^4J(H,H)= 2.1 Hz, 1H, H_4), 7.86 (m, 1H, $H_{4'}$), 7.62−7.60 (m, 8H, H_o), 7.45−7.42 (m, 8H, H_o), 7.35 (m, 3H, $H_{l/l'}$ and $H_{5'}$), 7.25−7.12 (m, 10H, H_p and H_g), 7.04−7.94 (m, 17H, H_m and H_k), 6.84 (d, ^3J(H,H) = 7.4 Hz, 2H, H_h), 6.71 (d, ^3J(H,H) = 8.2 Hz, 2H, $H_{l/l'}$), 2.67 (s, 8H, H_e and H_f). ^{13}C{^{1}H} NMR (75 MHz, CD_2Cl_2, ppm): δ 155.7 ($C_{2'}$), 154.3(C_2), 151.5 and 149.3 ($C_{6'}$ and C_6), 139.0 (C_4), 136.9 ($C_{4'}$) 136.9 (m, C_i), 134.3 (m, C_o), 134.1 (m, C_o), 131.3 (Cj), 131.0 (C_h), 130.5 (C_q) 130.0 and 129.9 (C_l and $C_{l'}$), 128.7(C_p), 128.6 (C_p), 127.5 (C_g), 127.1 (C_m), 122.8 (C_k), 122.0 ($C_{5'}$), 120.3 ($C_{3'}$), 120.0 (C_n), 119.3 (C_3), 116.3 and 114.8 (s, Ru−C≡*C*), 85.5 and 86.5 (s, C≡C−bipy), 31.5 (m, ^1J(P,C) + ^3J(P,C) = 24 Hz, P(CH_2)$_2$P). ^{31}P NMR (121 MHz, $CDCl_3$, ppm): δ 53.6 (s, PPh_2). IR (KBr, cm^{-1}): 2200 ($\nu_{C\equiv C}$) (m), 2051 ($\nu_{C\equiv C-Ru}$) (s). Anal. Found: C, 73.60; H, 4.92; N, 2.21. Calcd for [$C_{80}H_{64}N_2P_4Ru$]$_2$·CH_2Cl_2: C, 73.20; H, 4.96; N, 2.12. ESI-HRMS (*m*/*z*): [M + H]$^+$ 1279.3135 (calculated 1279.31363).

***trans*-[Ph−C≡C−(dppe)$_2$Ru−C≡C−C$_6$H$_4$−C≡C−bipy-κ^2*N*,*N*′−Yb(TTA)$_3$] (2Yb).** In a Schlenk tube, Yb(TTA)$_3$·2H_2O (35.0 mg, 0.041 mmol) and **2** (52.0 mg, 0.041 mmol) were dried under vacuum for 30 min and then dissolved in CH_2Cl_2 (23 mL). The red solution was stirred at ambient temperature for 16 h and then concentrated to ca. 3 mL under vacuum. After the addition of pentane (15 mL) an orange precipitate was separated by filtration, washed twice with pentane (2 mL), and dried under vacuum (57 mg, 66%). ^{1}H NMR (500 MHz, d_8-toluene, ppm): δ 26.55 (s, 1H, H_4), 26.00 (s, 1H, $H_{4'}$), 21 (bs, 1H, H_6 or $H_{6'}$), 16.91 (s, 1H, H_3), 16 (bs, 1H, H_6 or $H_{6'}$), 15.38 (s, 1H, $H_{3'}$), 11.30 (s, 1H, $H_{5'}$) 6.50−7.93 (m, 45H, H_{ar}), 6.45 (s, 3H, H_T), 5.32 (s, 3H, H_T), 2.99 (s, 3H, H_T), 2.39 (bs, 4H, H_e and H_f), 9.99 (bs, 3H, H_a). ^{31}P NMR (400 MHz, CD_2Cl_2, ppm): δ 52.9. IR (KBr, cm^{-1}): 2043 (s) ($\nu_{C\equiv C}$), 1630 (s) and 1604 (s) ($\nu_{C=O}$), 1180 (s) (ν_{C-F}). FAB$^+$-HRMS (*m*/*z*): [M]$^+$ 2015.1829 (calculated 2015.1792). Anal. Found for [$C_{96}H_{72}F_9N_2O_6P_4RuS_3Yb$]·2$CH_2Cl_2$: C, 53.80; H, 3.44; N, 1.35; S, 4.55. Calcd: C, 53.88; H, 3.51; N, 1.28; S, 4.40.

***trans*-[(dppe)$_2$Ru(−C≡C−bipy)$_2$] (3).** In a Schlenk tube, *cis*-$RuCl_2$(dppe)$_2$ (193 mg, 0.200 mmol), $NaPF_6$ (84 mg, 0,8 mmol), and 5-ethynyl-2,2′-bipyridine (90 mg, 0.5 mmol) were dried under vacuum for 30 min. Degassed dichloromethane (25 mL) was added with a syringe afterward. Then, triethylamine (0.45 mL) was added drop by drop. The mixture reacted at room temperature for 40 h, and then the solution was filtered and taken to dryness under vacuum. The residue was dissolved in dichloromethane (30 mL), washed with aqueous sodium hydrogenocarbonate (5 × 30 mL, pH 9), and dried (Na_2SO_4). The solvent was evaporated, and the residue was washed with pentane (2 × 30 mL) and dried to obtain an orange powder (189 mg, 0.15 mmol, 75%). ^{1}H NMR (400 MHz, $CDCl_3$, ppm): δ 8.65 (d, 2H, *J* = 1.5 Hz, H_6), 8.40 (d, 2H, *J* = 8 Hz, H_B), 8.17 (s, 2H, H_B), 8.12 (d, 2H, *J* = 8 Hz, H_B), 7.84 (t, 2H, *J* = 7.8 Hz, H_B), 7.50 (m, 16H, H_o), 7.19 (m, 8H, H_p), 6.95 (m, 16H, H_m), 2.72 (s, 8H, H_e and H_f). ^{13}C{^{1}H} NMR (75 MHz, CD_2Cl_2, ppm): δ 156.59 (s, $C_{2'}$), 150.23 (s, C_6), 149.58 (s, C_2), 149.03 (s, $C_{6'}$), 137.18 (s, C_4), 136.94, 136.67 (quintet, C_i), 136.57 (s, $C_{4'}$), 134.1 (s, C_o), 128.91 (s, C_p), 127.14 (s, C_m), 126.93 (s, C_5), 122.66 (s, $C_{5'}$), 120.27 (s, $C_{3'}$), 119.69 (s, C_3), 114.49 (s, Ru−C≡*C*), 31.4 (m, ^1J(P,C) + ^3J(P,C) = 24 Hz, P(CH_2)$_2$P). ^{31}P NMR (400 MHz, CD_2Cl_2, ppm): δ 54.6 (s, PPh_2). IR (KBr, cm^{-1}): $\nu_{C\equiv C}$ 2062 (s). UV−vis (CH_2Cl_2): 406 nm (ε = 31000 mol^{-1} L cm^{-1}). FAB$^+$-HRMS (*m*/*z*): [M + H]$^+$ 1257.3063 (calculated 1257.30457).

***trans*-[(dppe)$_2$Ru{−C≡C−C$_6$H$_4$−C≡C−bipy-κ^2*N*,*N*′−Yb(TTA)$_3$}$_2$] (3Yb).** In a Schlenk tube, Yb(TTA)$_3$·2H_2O (41.7 mg, 0.048 mmol) and *trans*-[Ru(dppe)$_2$(−C≡C−C_6H_4−C≡C−bpy)$_2$] (30.0 mg, 0.024 mmol) were dried under vacuum for 30 min and then dissolved in CH_2Cl_2 (5 mL). The red solution was stirred at ambient

dx.doi.org/10.1021/om500059d | *Organometallics* 2014, 33, 4824−4835

temperature for 16 h. A yellow precipitate was separated by filtration, washed twice with pentane (2 mL), and dried under vacuum (30 mg, 43%). The solubility of the product is too low in organic solvents to perform NMR measurements. IR (KBr, cm^{-1}): 2034 ($\nu_{C\equiv C-Ru}$) (s), 1630 and 1605 ($\nu_{C=O}$). Anal. Found: C, 50.89; H, 3.03; N, 1.92; S, 6.60. Calcd for $[C_{124}H_{86}N_4O_{12}F_{18}P_4S_6RuYb_2]$: C, 50.84; H, 2.96; N, 1.91; S, 6.57.

***trans*-[Cl−(dppe)$_2$Ru−(C═C═C$_{11}$H$_6$N$_2$)-κ^2*N*,*N*′−Yb(TTA)$_3$]OTf (4Yb).** In a Schlenk tube, Yb(TTA)$_3$·2H$_2$O (73 mg, 0.083 mmol) and *trans*-[Ru(dppe)$_2$Cl(C═C═C$_{11}$H$_6$N$_2$)]OTf (**4b**; 106 mg, 0.083 mmol) were dried under vacuum for 1 h and then dissolved in CH_2Cl_2 (20 mL). The obtained solution was stirred at ambient temperature for 16 h. After filtration, the solution was taken to dryness under vacuum. The residue was washed with pentane (3 × 5 mL). It was then recrystallized from dichloromethane and pentane (100 mg, 57%). ^{1}H NMR (500 MHz, CD_2Cl_2, ppm; all signals appear as broad peaks): δ 23.3 (2H), 15.3 (2H), 13.44 (8H, H_o), 11.59 (8H, H_o), 9.81 (8H, H_p), 8.54 (16H, H_m), 7.86 (4H, H_e or H_f), 7.26 (3H, H_T), 6.68 (4H, H_e or H_f), 5.92 (3H, H_T), 2.67 (3H, H_T), −17.33 (H_a); two protons from the diazafluorene part are not observed. ^{31}P NMR (400 MHz, CD_2Cl_2, ppm): δ 40.1 (bs). UV−vis: λ_{max} 447 nm (ε = 20620 L mol^{-1} cm^{-1}) and 532 nm (ε = 13170 L mol^{-1} cm^{-1}). IR (KBr, cm^{-1}): 1912 ($\nu_{C=C=C}$) (m), 1630 (s) 1603 (s) 1579 (s) ($\nu_{C=O}$), 1308, 1190, 1142 (ν_{C-F}) (s). Anal. Found: C, 50.81; H 3.08; N, 1.40; S, 6.09. Calcd for $[C_{90}H_{66}N_2O_6F_{12}P_4S_4RuYb]$: C, 51.25; H, 3.15; N, 1.33; S, 6.08.

■ ASSOCIATED CONTENT

Ⓢ Supporting Information

CIF files giving X-ray crystallographic data for **1**, **3**, **1Eu**, and **1Nd**. This material is available free of charge via the Internet at http://pubs.acs.org.

■ AUTHOR INFORMATION

Corresponding Author

*E-mail for S.R.: stephane.rigaut@univ-rennes1.fr.

Notes

The authors declare no competing financial interest.

■ ACKNOWLEDGMENTS

We thank the Université de Rennes 1, the CNRS, the ANR (RuOxLux-ANR-12-BS07-0010-01), and the Région Bretagne (Ph.D. grant for E.D.P.) for support. We are grateful to Dr.s Y. Guyot and A. Brenier (LPCML, University of Lyon) for their help in the NIR luminescence decay measurements and to Adrien Bourdolle (ENS Lyon) for his help in luminescence modulation experiments.

■ REFERENCES

(1) *Molecular Switches*; Feringa, B. L., Browne, W. R., Eds.; Wiley-VCH: Weinheim, Germany, 2011.

(2) Akita, M. *Organometallics* **2011**, *30*, 43. Liu, Y.; Hervault, Y.-M.; Ndiaye, C. M.; Norel, L.; Lagrost, C.; Rigaut, S. *Org. Lett.* **2012**, *14*, 4454. Lagrost, C.; Costuas, K.; Tchouar, N.; Le Bozec, H.; Rigaut, S. *Chem. Commun.* **2008**, 6117. Green, K. A.; Cifuentes, M. P.; Samoc, M.; Humphrey, M. G. *Coord. Chem. Rev.* **2011**, *255*, 2530. Samoc, M.; Gauthier, N.; Cifuentes, M. P.; Paul, F.; Lapinte, C.; Humphrey, M. G. *Angew. Chem., Int. Ed.* **2006**, *45*, 7376. Gauthier, N.; Argouarch, G.; Paul, F.; Toupet, L.; Ladjarafi, A.; Costuas, K.; Halet, J.-F.; Samoc, M.; Cifuentes, M. P.; Corkery, T. C. *Chem. Eur. J.* **2011**, *17*, 5561. Tanaka, Y.; Ishisaka, T.; Inagaki, A.; Koike, T.; Lapinte, C.; Akita, M. *Chem. Eur. J.* **2010**, *16*, 4762. Qi, H.; Gupta, A.; Noll, B. C.; Snider, G. L.; Lu, Y.; Lent, C.; Fehlner, T. P. *J. Am. Chem. Soc.* **2005**, *127*, 15218. Quardokus, R. C.; Lu, Y.; Wasio, N. A.; Lent, C. S.; Justaud, F.; Lapinte, C.; Kandel, S. A. *J. Am. Chem. Soc.* **2012**, *134*, 1710. Wasio, N. A.; Quardokus, R. C.; Forrest, R. P.; Corcelli, S. A.; Lu, Y.; Lent, C. S.; Justaud, F.; Lapinte, C.; Kandel, S. A. *J. Phys. Chem. C* **2012**, *116*, 25486. Marques-Gonzalez, S.; Yufit, D. S.; Howard, J. A. K.; Martin, S.; Osorio, H. M.; Garcia-Suarez, V. M.; Nichols, R. J.; Higgins, S. J.; Cea, P.; Low, P. J. *Dalton Trans.* **2013**, *42*, 338. Ying, J.-W.; Liu, I.P.-C.; Xi, B.; Song, Y.; Campana, C.; Zuo, J.-L.; Ren, T. *Angew. Chem., Int. Ed.* **2010**, *49*, 954. Green, K. A.; Cifuentes, M. P.; Corkery, T. C.; Samoc, M.; Humphrey, M.G. *Angew. Chem., Int. Ed.* **2009**, *48*, 7867.

(3) Rigaut, S. *Dalton Trans.* **2011**, *42*, 15859.

(4) Meng, F.; Hervault, Y.-M.; Shao, Q.; Hu, B.; Norel, L.; Rigaut, S.; Chen, X. *Nat. Commun.* **2014**, *5*, 3023. Meng, F.; Hervault, Y.-M.; Norel, L.; Costuas, K.; Van Dyck, C.; Geskin, V.; Cornil, J.; Hng, H. H.; Rigaut, S.; Chen, F. *Chem. Sci.* **2012**, *3*, 3113.

(5) Low, P. J. *Coord. Chem. Rev.* **2013**, *257*, 1517. Záliš, S.; Winter, R. F.; Kaim, W. *Coord. Chem. Rev.* **2010**, *254*, 1383. Costuas, K.; Rigaut, S. *Dalton Trans.* **2011**, *40*, 5643. Halet, J.-F.; Lapinte, C. *Coord. Chem. Rev.* **2013**, *257*, 1584. Aguirre-Etcheverry, P.; O'Hare, D. *Chem. Rev.* **2010**, *110*, 4839. Szafert, S.; Gladysz, J. A. *Chem. Rev.* **2006**, *106*, PR1. Bruce, M. I.; Low, P. J. *Adv. Organomet. Chem.* **2004**, *50*, 179.

(6) Kume, S.; Nishihara, H. *Dalton Trans.* **2008**, 3260.

(7) Tian, Z.; Li, A. D. Q. *Acc. Chem. Res.* **2013**, *46*, 269. Raymo, F. M. *Phys. Chem. Chem. Phys.* **2013**, *15*, 14840. Ko, C.-C.; Yam, V. W.-W. *J. Mater. Chem.* **2010**, *20*, 2063. Guerchais, V.; Ordronneau, L.; Le Bozec, H. *Coord. Chem. Rev.* **2010**, *254*, 2533.

(8) For examples see:. Seo, S.; Kim, Y.; Zhou, Q.; Clavier, G.; Audebert, P.; Kim, E. *Adv. Funct. Mater.* **2012**, *22*, 3556. Audebert, P.; Moimandre, F. *Chem. Sci.* **2013**, *4*, 575 and references therein.

(9) Xu, C.-H.; Sun, W.; Zhang, C.; Zhou, C.; Fang, C. J.; Yan, C. H. *Chem. Eur. J.* **2009**, *15*, 8717. Zapata, F.; Caballere, A.; Espinosa, A.; Tarraga, A.; Molina, P. *Dalton Trans.* **2009**, 3900. Yam, V. W.-W.; Roue, S.; Lapinte, C.; Fathallah, S.; Costuas, S.; Kahlal, S.; Halet, J.-F. *Inorg. Chem.* **2003**, *42*, 7086. Miomandre, F.; Stancheva, S.; Audibert, J.-F.; Brosseauy, A.; Paansu, R. B.; Lepeltier, M.; Mayer, C. R. *J. Phys. Chem. C* **2013**, *117*, 12806. Seo, S.; Pascal, S.; Park, C.; Shin, K.; Yang, X.; Maury, O.; Sarwade, B.; Andraud, C.; Kim, E. *Chem. Sci.* **2013**, *5*, 1538.

(10) Eliseeva, S. V.; Bünzli, J. C. G. *Chem.Soc. Rev.* **2010**, *39*, 189. dos Santos, C. M. G.; Harte, A. J.; Quinn, S. J.; Gunnlaugsson, T. *Coord. Chem.. Rev.* **2008**, *252*, 2512. Bünzli, J. C. G. *Chem. Rev.* **2010**, *110*, 2729. Moore, E. G.; Samuel, A. P. S.; Raymond, K. N. *Acc. Chem. Res.* **2009**, *42*, 542. Armelao, L.; Quici, S.; Barigelletti, F.; Accorsi, G.; Bottaro, G.; Cavazzini, M.; Tondello, E. *Coord. Chem. Rev.* **2010**, *254*, 487. Andraud, C.; Maury, O. *Eur. J. Inorg. Chem.* **2009**, 4357.

(11) Pandya, S.; Yu, J.; Parker, D. *Dalton Trans.* **2006**, 2757. Gunnlaugsson, T.; Leonnard, J. P. *Chem. Commun.* **2005**, 3114. Andrews, M.; Jones, J. E.; Harding, L. P.; Pope, J. A. *Chem. Commun.* **2011**, 206.

(12) Klink, S. I.; Keizer, H.; Van Veggel, F. C. J. M. *Angew. Chem., Int. Ed.* **2000**, *39*, 4319. Ward, M. D. *Coord. Chem. Rev.* **2007**, *251*, 1663. Chen, F.-N.; Chen, Z.-Q.; Bian, Z.-Q.; Huang, C.-H. *Coord. Chem. Rev.* **2010**, *254*, 991. Xu, H.-B.; Zhang, L.-Y.; Ni, J.; Chao, H.-Y.; Chen, Z.-N. *Inorg. Chem.* **2008**, *47*, 10744. Chen, Z.-N.; Fan, Y.; Ni, J. *Dalton Trans.* **2008**, 573. Kadjane, P.; Platas-Iglesias, C.; Ziessel, R.; Charbonniere, L. *Dalton Trans.* **2009**, 5688. Tropiano, M.; Record, C. J.; Morris, E.; Rai, H. S.; Allain, C.; Faulkner, S. *Organometallics* **2012**, *31*, 5673.

(13) D'Aléo, A.; Ouahab, L.; Andraud, C.; Pointillart, F.; Maury, O. *Coord. Chem. Rev.* **2012**, *256*, 1604.

(14) Yuan, Y.-F.; Cardinaels, T.; Lunstroot, K.; Van Hecke, K.; Van Meervelt, L.; Görller-Walrand, C.; Binnemans, K.; Nockemann, P. *Inorg. Chem.* **2007**, *46*, 5302. Pointillart, F.; Cauchy, T.; Maury, O.; Le Gal, Y.; Golhen, S.; Cador, O.; Ouahab, L. *Chem. Eur. J.* **2010**, *16*, 11226.

(15) Di Piazza, E.; Norel, L.; Costuas, K.; Bourdolle, A.; Maury, O.; Rigaut, S. *J. Am. Chem. Soc.* **2011**, *133*, 6174.

(16) (a) Norel, L.; Bernot, K.; Feng, M.; Roisnel, T.; Caneschi, A.; Sessoli, R.; Rigaut, S. *Chem. Commun.* **2012**, *48*, 3948. (b) Norel, L.; Min, F.; Bernot, K.; Roisnel, T.; Guizouarn, T.; Costuas, K.; Rigaut, S. *Inorg. Chem.* **2014**, *53*, 2361.

(17) Tropiano, M.; Kilah, N. L.; Morten, M.; Rahman, H.; Davis, J. J.; Beer, P. D.; Faulkner, S. *J. Am. Chem. Soc.* **2011**, *133*, 11847.

(18) Yano, M.; Matsuhira, K.; Tatsumi, M.; Kashiwagi, Y.; Nakamoto, M.; M Oyama, M.; Ohkubo, k.; Fukuzumi, S.; Misakifand, H.; Tsukube, H. *Chem. Commun.* **2012**, *48*, 4082.

(19) Sato, T.; Higushi, M. *Chem. Commun.* **2013**, *49*, 5256.
(20) Rigaut, S.; Perruchon, J.; Guesmi, S.; Fave, C.; Touchard, D.; Dixneuf, P. H. *Eur. J. Inorg. Chem.* **2005**, 447. Rigaut, S.; Maury, O.; Touchard, D.; Dixneuf, P. H. *Chem. Commun.* **2001**, 373. Mantovani, N.; Brugnati, M.; Gonsalvi, L.; Grigiotti, E.; Laschi, F.; Marvelli, L.; Peruzzini, M.; Reginato, G.; Rossi, R.; Zanello, P. *Organometallics* **2005**, *24*, 405.
(21) Olivier, C.; Kim, B.-S.; Touchard, D.; Rigaut, S. *Organometallics* **2008**, *27*, 509. Benameur, A.; Brignou, P.; Di Piazza, E.; Hervault, Y.-M.; Norel, L.; Rigaut, S. *New J. Chem.* **2011**, *35*, 2105.
(22) Grosshenny, V.; Roenero, F. M.; Ziessel, R. *J. Org. Chem.* **1997**, *62*, 1491. Schawb, P. F. H.; Fleischer, F.; Michl, J. *J. Org. Chem.* **2002**, *67*, 443.
(23) Vicente, J.; Gil-Rubio, J.; Barquero, N.; Jones, P. G.; Bautista, D. *Organometallics* **2008**, *27*, 646.
(24) Koutsantonis, G. A.; Jenkins, G. I.; Shauer, P. A.; Szczepaniak, B.; Skelton, B. W.; Tan, C.; White, A. H. *Organometallics* **2009**, *28*, 2195.
(25) It is important to note that these large molecules often contain included solvent (see Crystallographic Studies), precluding satisfactory elemental analysis. Importantly, ^{31}P NMR and electrochemical studies (vide infra) support the absence of unreacted materials or side products.
(26) Pélerin, O.; Olivier, C.; Roisnel, T.; Touchard, D.; Rigaut, S. *J. Organomet. Chem.* **2008**, *693*, 2153. Cifuentes, M. P.; Humphrey, M. G.; Koutsantonis, G. A.; Lengkeek, N. A.; Petrie, S.; Sanford, V.; Schauer, P. A.; Skelton, B. W.; Stranger, R.; White, A. H. *Organometallics* **2008**, *27*, 1716.
(27) Due to the paramagnetic nature of the complexes and their low solubility, ^{13}C NMR spectra with an acceptable *S*/*N* ratio could not be obtained.
(28) Freund, C.; Porzio, W.; Giovanella, U.; Vignali, F.; Pasini, M.; Destri, S.; Mech, A.; Di Pietro, S.; Di Bari, L.; Mineo, P. *Inorg. Chem.* **2011**, *50*, 5417. Zam, A.; Nozary, H.; Gune, L.; Besnard, C.; Lemmonier, J.-F.; Petoud, S.; Piguet, C. *Chem. Eur. J.* **2012**, *18*, 7155.
(29) Maury, O.; Viau, L.; Sénéchal, K.; Corre, B.; Guégan, J.-P.; Renouard, T.; Ledoux, I.; Zyss, J.; Le Bozec, H. *Chem.—Eur. J.* **2004**, *10*, 4454. Rendon, N.; Bourdolle, A.; Baldeck, P. L.; Le Bozec, H.; Andraud, C.; Brasselet, S.; Copéret, C.; Maury, O. *Chem. Mater.* **2011**, *23*, 3228.
(30) Bourdolle, A.; Allali, M.; D'Aléo, A.; Baldeck, P. L.; Kamada, K.; Williams, J. A. G.; Le Bozec, H.; Andraud, C.; Maury, O. *ChemPhysChem* **2013**, *14*, 3361.
(31) Ahmed, Z.; Iftikhar, K. *Inorg. Chim. Acta* **2010**, *363*, 2606. Pintacuda, G.; John, M.; Su, X.-C.; Otting, G. *Acc. Chem. Res.* **2007**, *40*, 206. Lapadula, G.; Bourdolle, A.; Allouche, F.; Conley, M.; del Rosal, I.; Maron, L.; Lukens, W. W.; Guyot, Y.; Andraud, C.; Brasselet, S.; Copéret, C.; Maury, O.; Andersen, R. A. *Chem. Mater.* **2014**, *26*, 1062.
(32) Younus, M.; Long, N. J.; Raithby, P. R.; Lewis, J.; Page, N. A.; White, A. J. P.; Williams, D. J.; Colbert, M. C. B.; Hodge, A. J.; Khan, M. S.; Parker, D. G. *J. Organomet. Chem.* **1999**, *578*, 198. Hurst, S. K.; Cifuentes, M. P.; Morrall, J. P. L.; Lucas, N. T.; Whittall, I. R.; Humphrey, M. G.; Asselberghs, I.; Persoons, A.; Samoc, M.; Luther-Davies, B.; Willis, A. C. *Organometallics* **2001**, *20*, 4664. Morrall, J. P.; Cifuentes, M. P.; Humphrey, M. G.; Kellens, R.; Robijns, E.; Asselberghs, I.; Clays, K.; Persoons, A.; Samoc, M.; W illis, A. C. *Inorg. Chim. Acta* **2006**, *359*, 998.
(33) Casanova, D.; Llunell, M.; Alemany, P.; Alvarez, S. *Chem. Eur. J.* **2005**, *11*, 1479.
(34) Llunell, M.; Casanova, D.; Cirera, J.: Bofill, J. M.; Alemany, P.; Alvarez, S. *SHAPE (version 2.1)*; Barcelona, 2013.
(35) Olivier, C.; Costuas, K.; Choua, S.; Maurel, V.; Turek, P.; Saillard, J.-Y.; Touchard, D.; Rigaut, S. *J. Am. Chem. Soc.* **2010**, *132*, 5638. Pevny, F.; Di Piazza, E.; Norel, L.; Drescher, M.; Winter, R. F.; Rigaut, S. *Organometallics* **2010**, *29*, 5912. Wuttke, E.; Pevny, F.; Hervault, Y.-M.; Norel, L.; Drescher, M.; Winter, R. F.; Rigaut, S. *Inorg. Chem.* **2012**, *51*, 1902.
(36) Gauthier, N.; Tchouar, N.; Justaud, F.; Argouarch, G.; Cifuentes, M. P.; Toupet, L.; Touchard, D.; Halet, J.-F.; Rigaut, S.; Humphrey, M. G.; Costuas, K.; Paul, F. *Organometallics* **2009**, *28*, 2253.
(37) Preliminary TD-DFT calculations were performed on the basis of the optimized structure of **1La** in ref 16b: Costuas, K.; Boilleau, C. Personal communication.
(38) Sénéchal, K.; Toupet, L.; Ledoux, I.; Zyss, J.; Le Bozec, H.; Maury, O. *Chem. Commun.* **2004**, 2180.
(39) Wang, B.; Wasielewski, M. R. *J. Am. Chem. Soc.* **1997**, *119*, 12. Sénéchal-David, K.; Hemeryck, A.; Tancrez, N.; Toupet, L.; Williams, J. A. G.; Ledoux, I.; Zyss, J.; Boucekkine, A.; Guégan, J.-P.; Le Bozec, H.; Maury, O. *J. Am. Chem. Soc.* **2006**, *128*, 12243.
(40) Shavaleev, N. M.; Pope, S. J. A.; Bell, Z. R.; Faulkner, S.; Ward, M. D. *Dalton Trans.* **2003**, 808−814. Shavaleev, N. M.; Scopelliti, R.; Gumy, F.; Bünzli, J.-C. G. *Eur. J. Inorg. Chem.* **2008**, 1523−1529. Shavaleev, N. M.; Accorsi, G.; Virgili, D.; Bell, Z. R.; Lazarides, T.; Calogero, G.; Armaroli, N.; Ward, M. D. *Inorg. Chem.* **2005**, *44*, 61−72.
(41) van Slageren, J.; Winter, R. F.; Klein, A.; Hartmann, S. *J. Organomet. Chem.* **2003**, *670*, 137.
(42) Reinhard, C.; Güdel, H. U. *Inorg. Chem.* **2002**, *41*, 1048. Pointillart, F.; Le Guennic, B.; Golhen, S. p.; Cador, O.; Maury, O.; Ouahab, L. *Inorg. Chem.* **2013**, *52*, 1610. Pointillart, F.; Guennic, B. L.; Golhen, S.; Cador, O.; Maury, O.; Ouahab, L. *Chem. Commun.* **2013**, *49*, 615. Cosquer, G.; Pointillart, F.; Jung, J.; Le Guennic, B.; Golhen, S.; Cador, O.; Guyot, Y.; Brenier, A.; Maury, O.; Ouahab, L. *Eur. J. Inorg. Chem.* **2014**, 69.
(43) Rigaut, S.; Monier, F.; Mousset, F.; Touchard, D.; Dixneuf, P. H. *Organometallics* **2002**, *21*, 2654.
(44) Beeby, A.; Faulkner, S.; Williams, J. A. G. *Dalton Trans.* **2002**, 1918. Ward, M. D. *Coord. Chem. Rev.* **2010**, *254*, 2634−2642 and references therein.
(45) Touchard, D.; Haquette, P.; Guesmi, S.; Le Pichon, L.; Daridor, A.; Toupet, L.; Dixneuf, P. H. *Organometallics* **1997**, *16*, 3640.
(46) Chaudret, B.; Commengues, G.; Poilblanc, R. *Dalton Trans.* **1984**, 1635.
(47) Lenaerts, P.; Ryckebosch, E.; Driesen, K.; Van Deun, R.; Nockemann, P.; Görler-Walrand, C.; Binnemans, K. *J. Lumin.* **2005**, *114*, 77. Melby, L. R.; Rose, N. J.; Abramson, E.; Caris, J. C. *J. Am. Chem. Soc.* **1964**, *86*, 5117.
(48) Connelly, N. G.; Geiger, W. E. *Chem. Rev.* **1996**, *96*, 877.
(49) Alternatively, the following procedure was used for the preparation of single crystals: $[Ln(TTA)_3{\cdot}2H_2O]$ (20 mg) was dissolved in boiling heptane (2 mL), the solution was cooled to 50 °C, and a solution of **1** (30 mg) in dichloromethane (2 mL) was added slowly. After filtration, the solution was cooled slowly to room temperature in a test tube. Small orange prisms formed upon cooling.